

ENGINEERING OF BIOMATERIALS

INŻYNIERIA BIOMATERIAŁÓW
CZASOPISMO POLSKIEGO STOWARZYSZENIA BIOMATERIAŁÓW
I WYDZIAŁU INŻYNIERII MATERIAŁOWEJ I CERAMIKI AGH

Number 102

Numer 102

Volume XIV

Rok XIV

JANUARY 2011

STYCZEŃ 2011

ISSN 1429-7248

PUBLISHER:

WYDAWCA:

**Polish Society
for Biomaterials
in Cracow**

Polskie
Stowarzyszenie
Biomateriałów
w Krakowie

EDITORIAL

COMMITTEE:

KOMITET

REDAKCYJNY:

Editor-in-Chief

Redaktor naczelny

Jan Chłopek

Editor

Redaktor

Elżbieta Pamuła

Secretary of editorial

Sekretarz redakcji

Design

Projekt

Katarzyna Trała

Augustyn Powroźnik

ADDRESS OF

EDITORIAL OFFICE:

ADRES REDAKCJI:

AGH-UST

30/A3, Mickiewicz Av.

30-059 Cracow, Poland

Akademia

Górnictwo-Hutnicza

al. Mickiewicza 30/A-3

30-059 Kraków

Issue: 200 copies

Nakład: 200 egz.

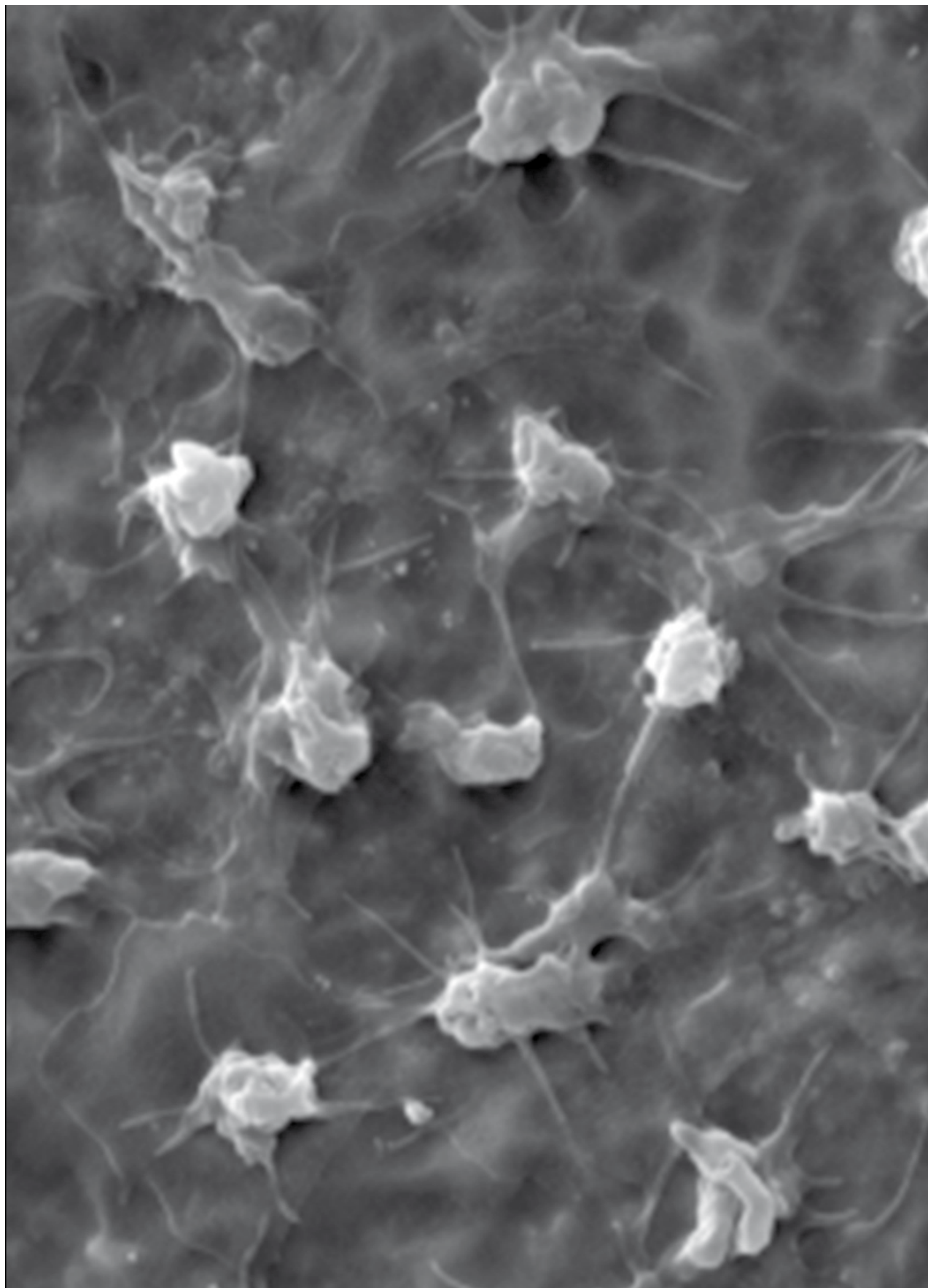
Scientific Publishing

House AKAPIT

Wydawnictwo Naukowe

AKAPIT

e-mail: wn@akapit.krakow.pl



INTERNATIONAL EDITORIAL BOARD
MIĘDZYNARODOWY KOMITET REDAKCYJNY

Iulian Antoniac

UNIVERSITY POLITEHNICA OF BUCHAREST, ROMANIA

Lucie Bacakova

ACADEMY OF SCIENCE OF THE CZECH REPUBLIC, PRAGUE, CZECH REPUBLIC

Romuald Będziński

POLITECHNIKA WROCŁAWSKA / WROCLAW UNIVERSITY OF TECHNOLOGY

Marta Błażewicz

AKADEMIA GÓRNICZO-HUTNICZA, KRAKÓW / AGH UNIVERSITY OF SCIENCE AND TECHNOLOGY, CRACOW

Stanisław Błażewicz

AKADEMIA GÓRNICZO-HUTNICZA, KRAKÓW / AGH UNIVERSITY OF SCIENCE AND TECHNOLOGY, CRACOW

Maria Borczuch-Łączka

AKADEMIA GÓRNICZO-HUTNICZA, KRAKÓW / AGH UNIVERSITY OF SCIENCE AND TECHNOLOGY, CRACOW

Wojciech Chrzanowski

UNIVERSITY OF SYDNEY, AUSTRALIA

Tadeusz Cieślik

ŚŁĄSKI UNIWERSYTET MEDYCZNY / MEDICAL UNIVERSITY OF SILESIA

Jan Ryszard Dąbrowski

POLITECHNIKA BIAŁOSTOCKA / BIAŁYSTOK TECHNICAL UNIVERSITY

Andrzej Górecki

WARSZAWSKI UNIWERSYTET MEDYCZNY / MEDICAL UNIVERSITY OF WARSAW

Robert Hurt

BROWN UNIVERSITY, PROVIDENCE, USA

James Kirkpatrick

JOHANNES GUTENBERG UNIVERSITY, MAINZ, GERMANY

Wojciech Maria Kuś

WARSZAWSKI UNIWERSYTET MEDYCZNY / MEDICAL UNIVERSITY OF WARSAW

Małgorzata Lewandowska-Szumieł

WARSZAWSKI UNIWERSYTET MEDYCZNY / MEDICAL UNIVERSITY OF WARSAW

Jan Marcinia

POLITECHNIKA ŚLĄSKA / SILESIAN UNIVERSITY OF TECHNOLOGY

Sergey Mikhalovsky

UNIVERSITY OF BRIGHTON, UNITED KINGDOM

Stanisław Mitura

POLITECHNIKA ŁÓDZKA / TECHNICAL UNIVERSITY OF LODZ

Roman Pampuch

AKADEMIA GÓRNICZO-HUTNICZA, KRAKÓW / AGH UNIVERSITY OF SCIENCE AND TECHNOLOGY, CRACOW

Stanisław Pielka

AKADEMIA MEDYCZNA WE WROCŁAWIU / WROCLAW MEDICAL UNIVERSITY

Vehid Salih

UCL EASTMAN DENTAL INSTITUTE, UNITED KINGDOM

Jacek Składzień

UNIWERSYTET JAGIELLOŃSKI, COLLEGIUM MEDICUM, KRAKÓW / JAGIELLONIAN UNIVERSITY, COLLEGIUM MEDICUM, CRACOW

Andrei V. Stanishevsky

UNIVERSITY OF ALABAMA AT BIRMINGHAM, USA

Anna Ślósarczyk

AKADEMIA GÓRNICZO-HUTNICZA, KRAKÓW / AGH UNIVERSITY OF SCIENCE AND TECHNOLOGY, CRACOW

Tadeusz Trzaska

AKADEMIA WYCHOWANIA FIZYCZNEGO, POZNAŃ / UNIVERSITY SCHOOL OF PHYSICAL EDUCATION, POZNAŃ

Dimitris Tsipas

ARISTOTLE UNIVERSITY OF THESSALONIKI, GREECE

Wskazówki dla autorów

1. Prace do opublikowania w kwartalniku „Engineering of Biomaterials / Inżynieria Biomateriałów” przyjmowane będą wyłącznie z tłumaczeniem na język angielski. Obcojęzyczność obowiązuje tylko język angielski.
2. Wszystkie nadsyłane artykuły są recenzowane.
3. Materiały do druku prosimy przysyłać na adres e-mail: kabe@agh.edu.pl lub Augustyn.Powroznik@agh.edu.pl
4. Struktura artykułu:
 - TYTUŁ • Autorzy • Streszczenie (100-200 słów) • Słowa kluczowe • Wprowadzenie • Materiały i metody • Wyniki i dyskusja • Wnioski • Podziękowania • Piśmiennictwo
5. Materiały ilustracyjne powinny znajdować się poza tekstem w oddzielnych plikach. Rozdzielczość rysunków min. 300 dpi. Wszystkie rysunki i wykresy powinny być czarno-białe lub w odcieniach szarości i ponumerowane cyframi arabskimi. W tekście należy umieścić odnośniki do rysunków i tabel. W tabelach i na wykresach należy umieścić opisy polskie i angielskie. W dodatkowym dokumencie należy zamieścić spis tabel i rysunków (po polsku i angielsku).
6. Na końcu artykułu należy podać wykaz piśmiennictwa w kolejności cytowania w tekście i kolejno ponumerowany.
7. Redakcja zastrzega sobie prawo wprowadzenia do opracowań autorskich zmian terminologicznych, poprawek redakcyjnych, stylistycznych, w celu dostosowania artykułu do norm przyjętych w naszym czasopiśmie. Zmiany i uzupełnienia merytoryczne będą dokonywane w uzgodnieniu z autorem.
8. Opinia lub uwagi recenzenta będą przekazywane Autorowi do ustosunkowania się. Nie dostarczenie poprawionego artykułu w terminie oznacza rezygnację Autora z publikacji pracy w naszym czasopiśmie.
9. Za publikację artykułów redakcja nie płaci honorarium autorskiego.
10. Adres redakcji:

Czasopismo
„Engineering of Biomaterials / Inżynieria Biomateriałów”
Akademia Górniczo-Hutnicza im. St. Staszica
Wydział Inżynierii Materiałowej i Ceramiki
al. Mickiewicza 30/A-3, 30-059 Kraków

tel. (48 12) 617 25 03, 617 22 38
tel./fax: (48 12) 617 45 41
e-mail: chlopek@agh.edu.pl,
kabe@agh.edu.pl,
Augustyn.Powroznik@agh.edu.pl,
www.biomat.krakow.pl

Warunki prenumeraty

Zamówienie na prenumeratę prosimy przysyłać na adres:
apowroz@agh.edu.pl, tel/fax: (48 12) 617 45 41
Konto:
Polskie Stowarzyszenie Biomateriałów
30-059 Kraków, al. Mickiewicza 30/A-3
Bank Śląski S.A. O/Kraków,
nr rachunku 63 1050 1445 1000 0012 0085 6001
Opłaty: cena pojedynczego numeru wynosi 20 PLN

Instructions for authors

1. Papers for publication in quarterly magazine „Engineering of Biomaterials / Inżynieria Biomateriałów” should be written in English.
2. All articles are reviewed.
3. Manuscripts should be submitted to Editor's Office by e-mail to kabe@agh.edu.pl, or Augustyn.Powroznik@agh.edu.pl
4. A manuscript should be organized in the following order:
 - TITLE • Authors and affiliations • Abstract (100-200 words) • Keywords (4-6) • Introduction • Materials and methods • Results and Discussions • Conclusions • Acknowledgements • References
5. Authors' full names and affiliations with postal addresses should be given. If authors have different affiliations use superscripts 1,2...
6. All illustrations, figures, tables, graphs etc. preferably in black and white or grey scale should be presented in separate electronic files (format .jpg, .gif, .tiff, .bmp) and not incorporated into the Word document. High-resolution figures are required for publication, at least 300 dpi. All figures must be numbered in the order in which they appear in the paper and captioned below. They should be referenced in the text. The captions of all figures should be submitted on a separate sheet.
7. References should be listed at the end of the article. Number the references consecutively in the order in which they are first mentioned in the text.
8. Opinion or notes of reviewers will be transferred to the author. If the corrected article will not be supplied on time, it means that the author has resigned from publication of work in our magazine.
9. Editorial does not pay author honorarium for publication of article.
10. Papers will not be considered for publication until all the requirements will be fulfilled.
11. Manuscripts should be submitted for publication to:

Journal
„Engineering of Biomaterials / Inżynieria Biomateriałów”
AGH University of Science and Technology
Faculty of Materials Science and Ceramics
30/A-3, Mickiewicz Av., 30-059 Cracow, Poland

tel. (48 12) 617 25 03, 617 22 38
tel./fax: (48 12) 617 45 41
e-mail: chlopek@agh.edu.pl,
kabe@agh.edu.pl,
Augustyn.Powroznik@agh.edu.pl
www.biomat.krakow.pl

Subscription terms

Subscription rates:
Cost of one number: 20 PLN
Payment should be made to:
Polish Society for Biomaterials
30/A3, Mickiewicz Av.
30-059 Cracow, Poland
Bank Slaski S.A. O/Krakow
account no. 63 1050 1445 1000 0012 0085 6001

XXI Conference on BIOMATERIALS IN MEDICINE AND VETERINARY MEDICINE

13-16 October 2011

Hotel "Perla Poludnia", Rytro

www.biomat.krakow.pl



SPIS TREŚCI

**ELASTIN AND COLLAGEN FIBRES ALTERATIONS
FOR ABDOMINAL AORTIC ANEURYSMS
POPULATION WITH CONSTANT MAXIMUM
DIAMETER SIZE**MAGDALENA KOBIELARZ, KRZYSZTOF MAKSYMOWICZ,
ROMUALD BĘDZIŃSKI

2

**FIBROBLAST BIOLOGICAL ACTIVITY ON
POLY(L-LACTIDE) AND POLY(L-LACTIDE-
CO-TRIMETHYLENE CARBONATE)**ANNA ŚCISŁOWSKA-CZARNECKA, ELŻBIETA PAMUŁA,
ELŻBIETA KOŁACZKOWSKA

7

**CHEMICAL MODIFICATION OF POLY
ε-CAPROLACTONE WITH WOLLASTONITE AND
ITS INFLUENCE ON BIOLOGICAL PROPERTIES
OF OSTEOBLAST LIKE-CELLS MG-63**ANNA ŚCISŁOWSKA-CZARNECKA, ELŻBIETA MENASZEK,
ELŻBIETA KOŁACZKOWSKA, MARTA BŁĄŻEWICZ,
JOANNA PODPORSKA

11

**BADANIA BIOLOGICZNE WARSTW
POWIERZCHNIOWYCH W ASPEKCIE
ZASTOSOWANIA NA PIERŚCIEN ZASTAWKI SERCA**M. GONSIOR, R. KUSTOSZ, T. BOROWSKI,
M. OSSOWSKI, M. SANAK, B. JAKIEŁŁA,
E. CZARNOWSKA, T. WIERZCHOŃ

15

**ANALIZA UWARUNKOWAŃ DECYDUJĄCYCH O
ODPORNOŚCI SZKLIWA NA ZUŻYCIE
CZĘŚĆ II: BADANIA WARSTWY WIERZCHNIEJ ORAZ
MIKROTWARDZOŚCI SZKLIWA ZĘBOWEGO**WOJCIECH RYNIIEWICZ, MARIOLA HERMAN,
ANNA M. RYNIIEWICZ

23

CONTENTS

**ELASTIN AND COLLAGEN FIBRES ALTERATIONS
FOR ABDOMINAL AORTIC ANEURYSMS
POPULATION WITH CONSTANT MAXIMUM
DIAMETER SIZE**MAGDALENA KOBIELARZ, KRZYSZTOF MAKSYMOWICZ,
ROMUALD BĘDZIŃSKI

2

**FIBROBLAST BIOLOGICAL ACTIVITY ON
POLY(L-LACTIDE) AND POLY(L-LACTIDE-
CO-TRIMETHYLENE CARBONATE)**ANNA ŚCISŁOWSKA-CZARNECKA, ELŻBIETA PAMUŁA,
ELŻBIETA KOŁACZKOWSKA

7

**CHEMICAL MODIFICATION OF POLY
ε-CAPROLACTONE WITH WOLLASTONITE AND
ITS INFLUENCE ON BIOLOGICAL PROPERTIES
OF OSTEOBLAST LIKE-CELLS MG-63**ANNA ŚCISŁOWSKA-CZARNECKA, ELŻBIETA MENASZEK,
ELŻBIETA KOŁACZKOWSKA, MARTA BŁĄŻEWICZ,
JOANNA PODPORSKA

11

**BIOLOGICAL PROPERTIES OF SURFACE
LAYERS FOR RING OF HEART VALVE
APPLICATION**M. GONSIOR, R. KUSTOSZ, T. BOROWSKI,
M. OSSOWSKI, M. SANAK, B. JAKIEŁŁA,
E. CZARNOWSKA, T. WIERZCHOŃ

15

**THE ANALYSIS OF ENAMEL RESISTANCE
TO WEAR DETERMINING FACTORS
PART II: STUDY OF SUPERFICIAL LAYER AND
MICROHARDNESS IN TOOTH ENAMEL**WOJCIECH RYNIIEWICZ, MARIOLA HERMAN,
ANNA M. RYNIIEWICZ

23

*STRESZCZANE W APPLIED MECHANICS REVIEWS
ABSTRACTED IN APPLIED MECHANICS REVIEWS**WYDANIE DOFINANSOWANE PRZEZ MINISTRA NAUKI
I SZKOLNICTWA WYŻSZEGO
EDITION FINANCED BY THE MINISTER OF SCIENCE
AND HIGHER EDUCATION*

ELASTIN AND COLLAGEN FIBRES ALTERATIONS FOR ABDOMINAL AORTIC ANEURYSMS POPULATION WITH CONSTANT MAXIMUM DIAMETER SIZE

MAGDALENA KOBIELARZ^{1,3*}, KRZYSZTOF MAKSYMOWICZ^{2,3}, ROMUALD BĘDZIŃSKI^{1,3}

¹ DIVISION OF BIOMEDICAL ENGINEERING AND EXPERIMENTAL MECHANICS, INSTITUTE OF MACHINE DESIGN AND OPERATION, FACULTY OF MECHANICAL ENGINEERING, WROCLAW UNIVERSITY OF TECHNOLOGY, POLAND

² DEPARTMENT OF FORENSIC MEDICINE, MEDICAL FACULTY, WROCLAW MEDICAL UNIVERSITY, POLAND

³ REGIONAL SPECIALIST HOSPITAL IN WROCLAW, RESEARCH AND DEVELOPMENT CENTRE, POLAND

* E-MAIL: MAGDALENA.KOBIELARZ@PWR.WROC.PL

Abstract

Development of abdominal aortic aneurysm (AAA) is a dynamic process proceeding as a result of the multi-factor pathological remodelling of elastin and collagen fibres, results an aneurysm expansion. In clinical practice, development of AAA is identified with aneurysm growth. Hence, the aim of this paper is to propose a taxonomy of load-bearing structural components alterations for AAA with relatively constant maximum diameter (average diameter 6.9 ± 0.8 cm). Structural investigations of normal ($n=47$) and aneurysmal ($n=46$) vessels were carried out on the basis of histological and ultrastructural examinations. The histological preparations were subjected to histometric evaluation; the number of collagen and elastin fibres and additionally the thickness of the particular vascular wall layers. A qualitative analysis of the abdominal aortic wall, mainly estimation of fibres arrangement, based on histological and ultrastructural (SEM) examinations were additionally performed. Using a cluster analysis, three stages of load-bearing fibres alterations for AAA population were distinguished. The clusters were systematized according to NAA results. For AAA population with relatively constant maximum diameter in the first stage of load-bearing fibres remodeling was observed a substantial loss of elastin fibres. The second stage is characterized by an increase in the number of collagen fibres. In the final stage the number of collagen is dramatically reduced. Presented results provide evidence to risk of AAA rupture is not connected with AAA size but a remodelling of extracellular matrix proteins. The remodelling is accompanied by changes in the AAA wall thickness, which should be taken into consideration when evaluating the degree of advancement of this disease.

Keywords: abdominal aorta, aneurysm, elastin fibres, collagen fibres, maximum diameter size, cluster analysis

[*Engineering of Biomaterials*, 102, (2011), 2-6]

Introduction

An abdominal aortic aneurysm (AAA) is a permanent and progressive dilatation of the abdominal aorta. The AAA occurs mainly in the infrarenal part of the abdominal aorta [1,2]. In the second half of the 20th century a dramatic increase (over sevenfold) in abdominal aortic aneurysm incidence occurred [3] and in the last 30 years just in the Eastern hemisphere the incidence has tripled [4]. The current number of persons with the AAA is not precisely known. The prevalence of the AAA in the different parts of the world largely depends on the age structure and the criteria used for classifying pathological changes. Hence AAA incidence may range from 1.2% to 27% [5]. Abdominal aortic aneurysm is a serious and potentially lethal condition. Aneurysm-associated mortality is the 13th most common cause of death in the western world [6,7]. Ruptured abdominal aortic aneurysm is associated with 50% to 90% mortality and most patients die before reaching hospital [8]. The frequency of AAA rupture has not decreased over time [9,10].

An abdominal aortic aneurysm arises as a result of the multifactorial pathologic remodelling of the aorta's connective tissue [11]. Many researches done in recent years indicate that the initiation, development and rupture of the aneurysm are caused by the degradation of the load-bearing structural components of an aortic wall, i.e. elastin and collagen fibres [12-16], induced by proteolytic enzymes from the endopeptidase family, represented mainly by matrix metalloproteinases (MMPs) [1,17]. It has been found a variable degree of reduction in the content of elastic fibres in the walls of abdominal aortic aneurysms [18-22]. The amount of collagen fibres in the AAA wall may increase [20,23], remain unchanged [24] or decrease [1,25]. The variety of the connective tissues fibres content may be justified by different levels of aneurysm development. Thompson and Baxter [17,26] were the first to describe the structural alterations taking place in the abdominal aortic wall in the course of growth of the aneurysm, because the AAA maximum diameter size is used in clinical practice as an indication for aneurysm surgery [9] since it is thought that the probability of rupture of an AAA increases with its diameter [1,27]. However, as research shows, AAA may rupture regardless of the vessel's diameter. The aneurysm may rupture even in the case of vessels with a diameter less than 40 mm in which hypothetically the risk is the lowest [8], while there are cases when aneurysms expand, reaching sizes larger than 80 mm without any signs of rupturing [28]. Hence, the aim of this paper is to propose a classification (taxonomy) of elastin and collagen fibres alterations for abdominal aortic aneurysms with relatively constant maximum diameter due to eliminate growth factor in analysis. We advance a hypothesis that for AAAs with comparable maximum diameter, degree of load-bearing structural components alterations may be significantly different.

Material and methods

Experimental material

The experimental material was obtained at surgical infrarenal abdominal aorta aneurysm walls (AAA) resection and normal abdominal aortas (NAA) autopsy. The AAAs walls were intraoperatively harvested from 46 patients (34 male, 12 female, average age: 68 ± 9 years). Average diameter of AAA were relatively constant and amounted to 6.9 ± 0.8 cm. Due to restrictions of surgical AAA resection and to avoid the differences between parts of the aneurysm, vascular walls samples were taken from the anterior region of the AAAs only. The NAA walls were taken during autopsies from 47 age-matched donors (39 male, 8 female, average age: 66 ± 11 years, average diameter: 2.4 ± 0.5 cm).

Histological and ultrastructural examinations

For the purpose of histological analysis, vascular wall segments 10 mm² in area were fixed in a 4% buffered formalin solution for 48 hours, washed under running water, dehydrated through ascending grades of alcohol, cleared in methyl benzoate and xylene, consecutively, and then embedded in paraffin wax, according to routine techniques. The paraffin-embedded tissues were sectioned into 5 µm thickness. The slides were stained routinely with hematoxylin and eosin according to Delafield, Verhoff's and van Gieson method. The sections stained with Verhoff's and Van Gieson's method were subjected to histometric analysis. The collagen and elastin fibres were counted. A single slide was divided into 10 sections along which all the fibres that the drawn lines intersected were counted. Measurements of the overall wall thickness of the investigated vessels and the thickness of the layers (the intima, the media and the adventitia) were performed. The results of the histometric calculations were averaged for each investigated preparation. The stained preparations were viewed with a light microscope (*Axiomager M1m*, Zeiss).

Aortic wall fragments 10 mm² in area constituted the material for ultrastructural examinations. The experimental material was fixed in a 2.5% phosphate-buffered glutaraldehyde, dehydrated in an acetone series, then dried and stuck onto microscope stages, using carbon glue. For the purpose of ultrastructural analysis the previously dried material had to be sprayed with gold. The preparations were viewed under a scanning electron microscope (*Leo 435 VP*, Zeiss) and the image was recorded in high vacuum.

Statistical analysis

The histometric results were subjected to statistical analysis (*Statistica 8.0*, StatSoft). The results were presented in the form of averages with standard deviations ($\bar{X} \pm \text{SD}$). The statistical analysis of the data was based on Student's t-test for independent samples. The statistical tests were carried out to a significance level (p) of 0.05.

Cluster analysis

The cluster analysis (*Statistica 8.0*, StatSoft) was used to group into sets the histometric measurements for taxonomic purposes. This method enables to group the results into sets (clusters) comprising data with the highest degree of similarity and maximally different from one to another. Number of sets for the AAA population were adopted as 3 likewise like Thompson and Baxter findings [17,26].

Results

Histological examinations

No significant pathological changes were found in the histological images of the healthy abdominal aortic walls. No atrophy or significant structural disorders were observed in them. Numerous elastin fibres (E) were present within the aortic media of the NAA walls (FIG. 1a,b).

TABLE 1. Average number of elastin and collagen fibres in walls of normal abdominal aortas (NAA) and abdominal aortic aneurysms (AAA).

| | | Average | SD |
|-----|---------------------|---------|------|
| NAA | Elastin fibres (E) | 54.2 | 9.8 |
| | Collagen fibres (K) | 83.8 | 10.9 |
| AAA | Elastin fibres (E) | 9.1 | 6.2 |
| | Collagen fibres (K) | 45.8 | 38.4 |

The collagen fibres (K) observed in both the aortic media and the adventitia were morphologically normal (wavy). Their number varied between the preparations, but the differences were not considerable (TABLE 1).

In the histological images of the abdominal aortic aneurysm walls numerous pathological changes were discovered (FIG. 1). All the abdominal aortic aneurysm walls were characterized by a considerable reduction in the number of elastin fibres (E) in the media (TABLE 1). Extremely variable amount of elastin fibres (E) randomly occurred in the full histological picture of the aneurysm walls (FIG. 1c). In a few cases, elastin fibres fragmentation was observed (FIG. 1d). The measurements of elastin fibres number were not performed for these cases. The number of collagen fibres (K) in the abdominal aortic aneurysm walls was found to be reduced, but the size of the reduction varied between individual cases. The arrangement of collagen fibres in the media of the AAA walls was disordered.

On average, the reduction in the number of elastin and collagen fibres in the AAA walls, in comparison with the results obtained for the normal abdominal aortas, was statistically significant with significance levels $p=0.000001$ and $p=0.0059$, respectively.

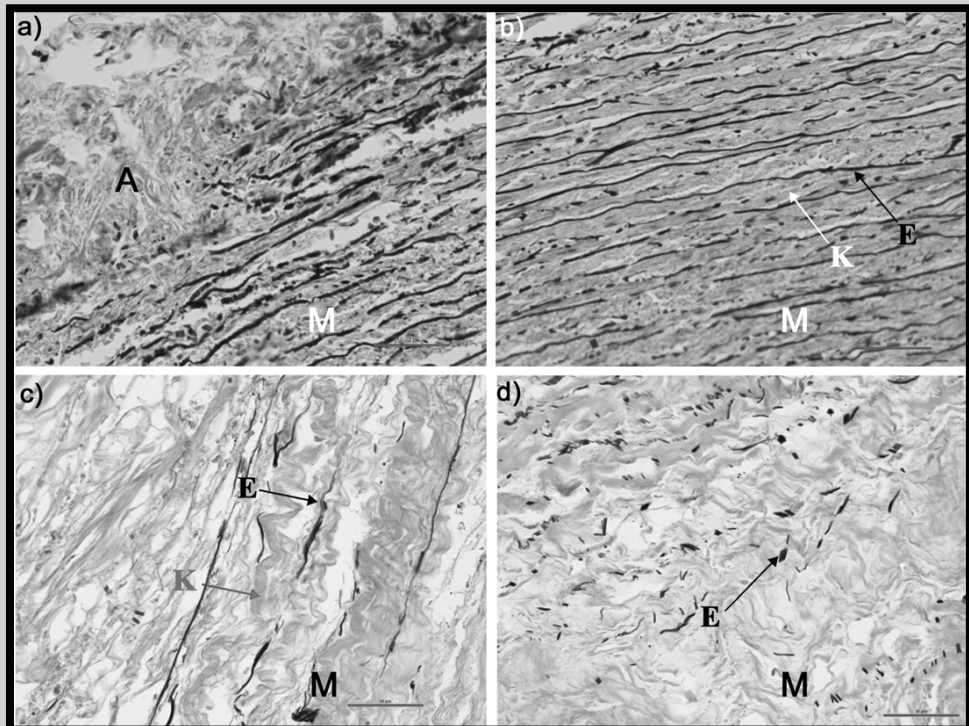


FIG. 1. Histological images of normal abdominal aortic walls (NAA) and abdominal aortic aneurysm walls (AAA): a) NAA wall (A – adventitia, M – media) according Verhoff's stain, b) elastin (E) and collagen (K) fibres in histological image of NAA wall media (Verhoff's stain), c) single elastin fibre (E) in AAA wall (Van Gieson's stain), d) fragmentation of elastin fibres (E) in AAA wall media (Van Gieson's stain). Reprinted with permission from [29].

TABLE 2. Wall thickness of normal abdominal aortas (NAA) and abdominal aortic aneurysms (AAA) and that of their individual constitutive layers.

| | | Average [μm] | SD [μm] |
|------------|-------------------------------|------------------------------|-------------------------|
| NAA | Intima (I) | 272 | 81 |
| | Media (M) | 722 | 202 |
| | Adventitia (A) | 202 | 52 |
| | Overall wall thickness | 1196 | 335 |
| AAA | Intima (I) | 63 | 23 |
| | Media (M) | 674 | 347 |
| | Adventitia (A) | 194 | 105 |
| | Overall wall thickness | 931 | 475 |

All the layers of the abdominal aortic aneurysm walls were normally formed. The boundaries between the layers were distinct whereby the thickness of the latter could be precisely determined (TABLE 2). In most cases, the boundaries between the AAA wall layers had become blurred. Disorders in the laminar structure were observed. The thickness of the particular layers in the abdominal aortic aneurysm walls was difficult to measure. It could be measured only in the cases when their boundaries were discernible in the histological images (TABLE 2).

The statistical analysis showed that the wall thickness of the aneurysms becomes reduced relative to that of the normal abdominal aortas ($p=0.02$). The largest reduction (about 80% as regards average values) occurs in the case of the tunica intima ($p=0.0015$).

Ultrastructural examinations

The characteristic morphologically normal arrangement of fibres (forming a three-dimensional network) was observed in SEM images of the normal abdominal aortic walls (FIG. 2a). SEM images of the abdominal aortic aneurysm walls showed that the shape of collagen fibres in the adventitia was disordered and in most of the examined cases it was almost straight-linear (FIG. 2b).

Load-bearing fibres alterations for AAAs with relatively constant diameter

AAAs population with relatively constant diameter had to be grouped into sets on the basis of the histometric measurements by used the cluster analysis. The sets were systematized and normalized to NAA results. Three main stages of load-bearing fibres remodeling for abdominal aortic aneurysm population with relatively constant diameter were distinguished by different structural parameters (FIG. 3). No differences were observed between AAA diameter in particular sets.

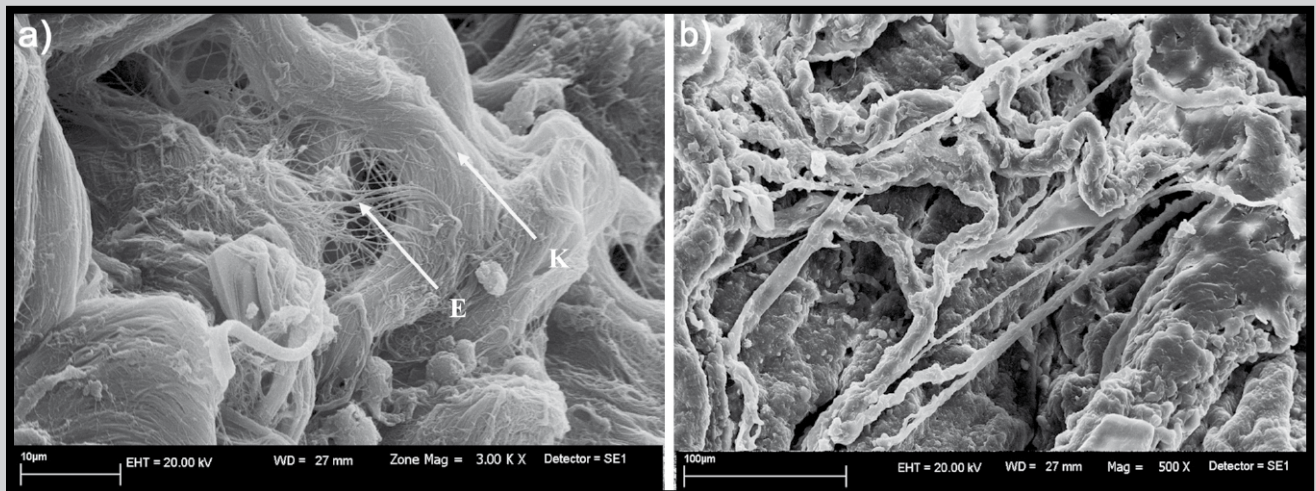


FIG. 2. SEM images of walls of normal abdominal aortas (NAA) and abdominal aortic aneurysms (AAA): a) elastin (E) and collagen (K) fibres in NAA wall media; b) straight-linear shape of collagen fibres in adventitia of AAA. Reprinted with permission from [29].

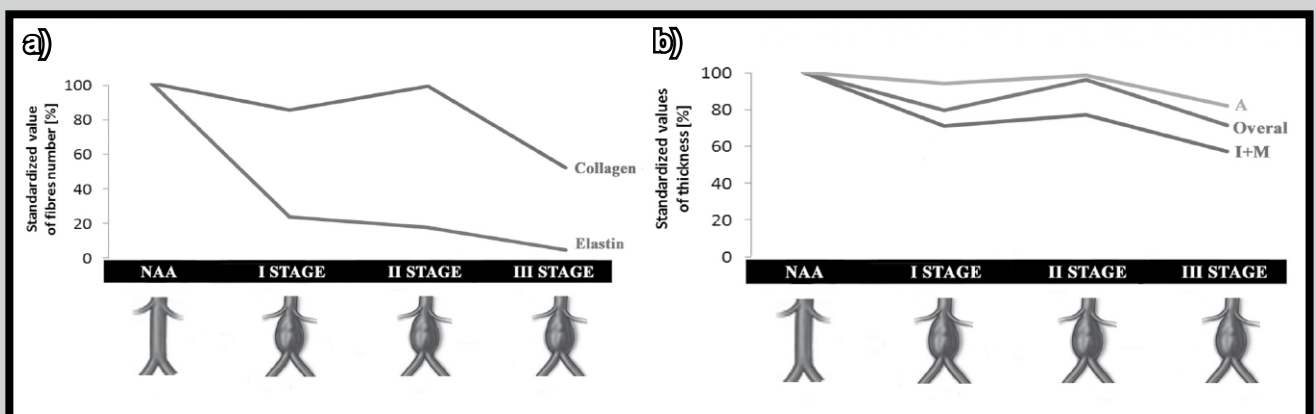


FIG. 3. Structural parameters alterations for AAAs population with relatively constant diameter: a) load-bearing fibres and b) thickness of adventitia (A), media (M) and overall aortic wall (Overall).

The walls of the abdominal aortic aneurysms in the first stage are characterized by a considerable reduction in the number of elastin fibres relative to their number in the walls of the normal aortas. No significant reduction in the number of collagen fibres was observed. No distinct anomalies were found in the walls of the aneurysms. The thickness of all the aneurysm wall layers underwent insignificant reduction (the intima was still discernible). The second stage is characterized by inflammatory infiltrations and numerous newly formed vasa vasorum (neovascularization) were commonly observed in the histological and SEM images of the walls of the aneurysms. An increase in the number of collagen fibres relative to their number in the preceding stage was observed. As the activity of the collagen fibres and their production intensify, the thickness of the AAA wall increases (mainly in adventitia and media part). However, no intima was found in the histological images of the aneurysm walls. In the final stage the number of collagen is dramatically reduced. In most of the analyzed cases, the spaces between collagen fibres were filled with thrombuses. The wall thickness was much reduced in comparison with the preceding stage.

Discussion

The development of the abdominal aortic aneurysm leading to the rupture of its wall can be considered as a classical case of material failure due to excessive loading, the insufficient strength of the material or the two factors combined [30]. The underlying process is the remodelling of the structural elements which bear mechanical loads, i.e. elastin and collagen fibres [14-16]. It has been found that the concentration of elastic fibres in the walls of abdominal aortic aneurysms undergoes considerable reduction [18-22]. Roughly about 63-92% of the elastin fibres are lost [31]. The amounts of collagen fibres in the AAA wall may increase [20,23], remain unchanged [24] or decrease [1,25]. The discrepancies between the results obtained by the cited authors are justified since remodelling which takes place in the abdominal aortic aneurysm wall is considered as a dynamic process. According to the best of our knowledge the unique AAA development identification model were proposed by Thompson and Baxter [17,26]. They proposed three-stage taxonomy of characteristic structural changes in relation to the aneurysm's maximum diameter. We propose a new classification of load-bearing elements alteration based on histometric measurements carried out for a large group of asymptomatic abdominal aneurysm with a constant maximum diameter (average diameter 6.9 ± 0.8 cm). We no longer take into account the maximum aneurysm diameter as the main aneurysm development parameter, but degree of elastin and collagen remodeling. First elastin fibres undergo fragmentation and their concentration in the aortic wall media decreases. As a result of the degradation of the elastin fibres in the media the vessel's capacity to carry tensile stresses decreases and collagen production is triggered. In the second stage, for the sake of progressive elastin fibres degradations collagen fibres behave compensatory and the taking over of the elastin fibres' load bearing function by them. The third stage is characterized by decreases of the collagen fibres content in the vascular wall so does the latter's tensile strength, which is the main cause of rupture of the aneurysm. This corroborates the thesis proposed earlier that the loss of elastin fibres in the AAA wall is connected mainly with the development of the aneurysm while the breaking of AAA wall continuity is linked with the degradation of collagen fibres [25,32,33]. Presented results provide evidence to risk of AAA rupture is not connected with AAA size but a remodelling of extracellular matrix proteins.

The presented results indicate that the thickness of the aneurysm wall and that of its individual layers change with the changes taking place in the wall structure. Measurements of intima – media thickness is existing in clinical practise as predictor of arteriosclerosis diagnosis and development [34]. In clinical conditions vascular wall thickness can be measured (similarly as the AAA diameter) using non-invasive diagnostic techniques (e.g. ultrasonography or computer tomography). The use of the new parameter (AAA wall thickness) for evaluating the degree of advancement of an aneurysm requires further research, although, as indicated by using cluster analysis, it is theoretically possible to correlate AAA wall thickness with the number of fibres and the condition of the vessel's tissue.

This study has some limitations. Firstly, due to restrictions associated with open surgical procedures, the current results were derived from AAA wall samples from the anterior region of the AAA only. Hence, samples should be obtained from the anterior, posterior, and both lateral regions of AAA due to most AAAs are asymmetric as a result of the local support provided by lumbar vertebrae. Furthermore, abdominal aortic aneurysm rupture is observed to occur at a greater rate at the posterior wall than the anteriorly [35]. Recent reports on the variability in AAA wall strength as a function of location [36] suggest this may be one of a few factors to consider whenever using in presented classification. Secondly, number of elastin and collagen fibers only were considered. Evaluation of fibers arrangement influences on AAA development were not discussed. One can expect that the arrangement is significant as the fibers number [37]. Three-dimensional fibers arrangement was analyzed only in scanning electron microscopy, although we did not obtain quantitative results by this method. Some limitation of our study is fact that semi-quantifications of elastin and collagen were done through histology, which permits only histometric measurements of elastin and collagen content in 2D imaging. Biochemical assay could improve the knowledge about total quantity of elastin and collagen fibres in tissue volume. However, the results of biochemical assays are in general agreement with our results [25,31-33]. Additionally, histological examinations provide more information about associate phenomenon, like inflammatory or neovascularization processes, which could be connected with the degradation of elastin and collagen fibres [38-40]. Our histological examinations of the walls of aneurysms revealed extensive inflammatory infiltrations in most of the cases (presented in [29]). The inflammatory infiltrations are composed mainly of B lymphocytes, T cells and macrophages [6,41]. The inflammatory cells in the media and in the adventitia come directly from the blood which is supplied to the wall by the newly forming (as a result of intensified neovascularization characteristic of this pathology) vessels of the vessels (*vasa vasorum*) [1]. In the histological images of the abdominal aortic aneurysm walls all of them were discovered (presented in [29]).

Acknowledgements

This publication is part of project „Wrovasc – Integrated Cardiovascular Centre”, co-financed by the European Regional Development Fund, within Innovative Economy Operational Program, 2007-2013.

References

- [1] Sakalihasan, N., R. Limet, and O. Defawe, Abdominal aortic aneurysm. *Lancet*, 2005; 365: 1577-89.
- [2] Li, Z. and C. Kleinstreuer, Analysis of biomechanical factors affecting stent-graft migration in an abdominal aortic aneurysm model. *J Biomech*, 2006; 39: 2264-2273.
- [3] Geest, J., M. Sacks, and D. Vorp, A planar biaxial constitutive relation for the luminal layer of intra-luminal thrombus in abdominal aortic aneurysms. *J Biomech*, 2006; 39: 2347-2354.
- [4] Bosch, J., J. Lester, P. McMahon, M. Beinfeld, E. Halpern, J. Kaufman, D. Brewster, and G. Gazelle, Hospital costs for elective endovascular and surgical repairs of infrarenal abdominal aortic aneurysms. *Radiology*, 2001; 220: 492-497.
- [5] Softysiak, A., Tętniaki aorty brzusznej. 2000, Łódź: Drukarnia Wydawnictw Naukowych S.A.
- [6] Choke, E., G. Cockerill, W. Wilson, S. Sayed, J. Dawson, I. Loftus, and M. Thompson, A review of biological factors implicated in abdominal aortic aneurysm rupture. *Eur J Vasc Endovasc Surg*, 2005; 30: 227-244.
- [7] Patel, M., D. Hardman, C. Fisher, and M. Appleberg, Current views on the pathogenesis of abdominal aortic aneurysms. *J Am Coll Surgeons*, 1995; 181: 371-382.
- [8] Vliet, A. and A. Boll, Abdominal aortic aneurysm. *Lancet*, 1997; 349: 863-66.
- [9] Hans, S., O. Jareunpoon, M. Balasubramaniam, and G. Zeleznock, Size and location of thrombus in intact and ruptured abdominal aortic aneurysms. *J Vasc Surg*, 2005; 41: 584-588.
- [10] Noel, A., P. Gloviczki, K. Cherry, T. Bower, J. Panneton, and G. Mozes, Ruptured abdominal aortic aneurysm; the excessive mortality of conventional repair. *J Vasc Surg*, 2001; 34: 41-46.
- [11] Davies, M., Aortic aneurysm formation: lessons from human studies and experimental models. *Circulation*, 1998; 98: 193-195.
- [12] Longo, M., S. Buda, N. Fiotta, W. Xiong, T. Griener, S. Shapiro, and T. Baxter, MMP-12 has a role in abdominal aortic aneurysms in mice. *Surgery*, 2005; 137: 457-462.
- [13] Eriksson, P., K. Jones, L. Brown, R. Greenhalgh, A. Hamsten, and J. Powell, Genetic approach to the role of cysteine proteases in the expansion of abdominal aortic aneurysms. *Brit J Surg*, 2004; 91: 86-89.
- [14] Shteinberg, D., M. Halak, S. Shapiro, A. Kinarty, E. Sobol, N. Lahat, and R. Karmeli, Abdominal aortic aneurysm and aortic occlusive disease: a comparison of risk factors and inflammatory response. *Eur J Vasc Endovasc Surg*, 2000; 20: 462-465.
- [15] Panek, B., M. Gacko, and J. Pałka, Metalloproteinases, insulin-like growth factor-I and its binding proteins in aortic aneurysm. *Int J Exp Pathol*, 2004; 85: 159-164.
- [16] Robicsek, F., M. Thubrikar, and A. Fokin, Cause of degenerative disease of the trileaflet aortic valve: review of subject and presentation of a new theory. *Ann Thorac Surg*, 2002; 73: 1346 - 1354.
- [17] Thompson, R. and T. Baxter, MMP Inhibition in abdominal aortic aneurysms rationale for a prospective randomized clinical trial. *Ann NY Acad Sci*, 1999; 878: 159-178.
- [18] MacSweeney, S., J. Powell, and R. Greenhalgh, Pathogenesis of abdominal aortic aneurysm. *Brit J Surg*, 1994; 82: 935.
- [19] Powell, J. and R. Greenhalgh, Cellular, enzymatic and genetic factors in the pathogenesis of abdominal aortic aneurysms. *J Vasc Surg*, 1989; 9: 297-304.
- [20] He, C. and M. Roach, The composition and mechanical properties of abdominal aortic aneurysms. *J Vasc Surg*, 1994; 20: 6-13.
- [21] Jacob, T., E. Ascher, A. Hingorani, Y. Gunduz, and S. Kallakuri, Initial steps in the unifying theory of the pathogenesis of artery aneurysms. *J Surg Res*, 2001; 101: 37-43.
- [22] MacSweeney, S., G. Young, R. Greenhalgh, and J. Powell, Mechanical properties of the aneurysmal aorta. *Brit J Surg*, 1992; 79: 1281-1284.
- [23] Eugster, T., A. Huber, T. Obeid, I. Schwegler, L. Gurke, and P. Stierli, Aminoterminal propeptide of type III procollagen and matrix metalloproteinases-2 and -9 failed to serve as serum markers for abdominal aortic aneurysm. *Eur J Vasc Endovasc Surg*, 2005; 29: 378-382.
- [24] McGee, G., T. Baxter, V. Shively, R. Chisholm, W. McCarthy, W. Flinn, J. Yao, and W. Pearce, Aneurysm or occlusive disease - factors determining the clinical course of atherosclerosis of the infrarenal aorta. *Surgery*, 1991; 110: 370- 375.
- [25] Damme, H., N. Sakalihasan, and R. Limet, Factors promoting rupture of abdominal aortic aneurysms. *Acta Chir Belg*, 2005; 105: 1-11.
- [26] Thompson, R., P. Geraghty, and J. Lee, Abdominal aortic aneurysms: basic mechanisms and clinical implications. *Curr Prob Surg*, 2002; 39: 93-232.
- [27] Finlayson, S., J. Birkmeyer, M. Fillinger, and J. Cronenwett, Should endovascular surgery lower the threshold for repair of abdominal aortic aneurysms? *J Vasc Surg*, 1999; 29: 973-85.
- [28] Raghavan, M. and D. Vorp, Toward a biomechanical tool to evaluate rupture potential of abdominal aortic aneurysm: identification of a finite strain constitutive model and evaluation of its applicability. *J Biomech*, 2000; 33: 475-482.
- [29] Kobielarz, M., K. Maksymowicz, K. Kaleta, P. Kuropka, K. Marycz, and R. Będziński, Histological and ultrastructural evaluation of the walls of abdominal aortic aneurysms. *Engineering of Biomaterials*, 2010; 13: 83-87.
- [30] Sonesson, B., F. Hansen, and T. Lanne, Abdominal aortic aneurysm: a general defect in the vasculature with focal manifestations in the abdominal aorta. *J Vasc Surg*, 1997; 26: 247-254.
- [31] Watton, P., N. Hill, and M. Heil, A mathematical model for the growth of the abdominal aortic aneurysm. *Biomech Model Mechan*, 2004; 3: 98-113.
- [32] Chang, M. and M. Roach, The composition and mechanical properties of abdominal aortic aneurysms. *J Vasc Surg*, 1994; 20: 6-13.
- [33] Wills, A., M. Thompson, M. Crowther, R. Sayers, and P. Bell, Pathogenesis of abdominal aortic aneurysms - cellular and biochemical mechanisms. *Eur J Vasc Endovasc Surg*, 1996; 12: 391-400.
- [34] Simon, A., J.-L. Megnien, and G. Chironi, The value of carotid intima-media thickness for predicting cardiovascular risk. *Arterioscl Throm Vas*, 2010; 30: 182.
- [35] Darling, R., C. Messina, D. Brewster, and L. Ottinger, Autopsy study of unoperated abdominal aortic aneurysms. *Circulation*, 1977; 56: 161-164.
- [36] DiMartino, E. and D. Vorp, Effect of variation in intraluminal thrombus constitutive properties on abdominal aortic aneurysm wall stress. *Ann Biomed Eng*, 2003; 31: 804-809.
- [37] Hanuza, J., M. Mączka, M. Gąsior-Głogowska, M. Komorowska, M. Kobielarz, R. Będziński, S. Szótek, K. Maksymowicz, and K. Hermanowicz, FT-Raman spectroscopic study of thoracic aortic wall subjected to uniaxial stress. *J Raman Spectrosc*, 2009; 40: 1163-1169.
- [38] Thompson, M. and G. Cockerill, Matrix Metalloproteinase-2 the forgotten enzyme in aneurysm pathogenesis. *Ann NY Acad Sci*, 2006; 1085: 170-174.
- [39] Brady, A., S. Thompson, G. Fowkes, R. Greenhalgh, and J. Powell, Abdominal aortic aneurysm expansion. Risk factors and time intervals for surveillance. *Circulation*, 2004; 110: 16-21.
- [40] Grygier, D., P. Kuropka, and W. Dudziński, Microscopic and histological analysis of the processes occurring in the aperture and wall of a coronary vessel after stent implantation. *Acta Bioeng Biomech*, 2008; 10: 55-60.
- [41] Bobryshev, Y., R. Lord, and H. Parsson, Immunophenotypic analysis of the aortic aneurysm wall suggests that vascular dendritic cells are involved in immune responses. *Cardiovasc Surg*, 1998; 6: 240-249.

FIBROBLAST BIOLOGICAL ACTIVITY ON POLY(L-LACTIDE) AND POLY(L-LACTIDE-CO-TRIMETHYLENE CARBONATE)

ANNA ŚCISŁOWSKA-CZARNECKA¹, ELŻBIETA PAMUŁA²,
ELŻBIETA KOŁACZKOWSKA³

¹ACADEMY OF PHYSICAL EDUCATION,
FACULTY OF ANATOMY, KRAKOW, POLAND

²AGH UNIVERSITY OF SCIENCE AND TECHNOLOGY, FACULTY
OF MATERIALS SCIENCE AND CERAMICS, KRAKOW, POLAND

³JAGIELLONIAN UNIVERSITY, DEPARTMENT OF EVOLUTIONARY
IMMUNOBIOLOGY, INSTITUTE OF ZOOLOGY, KRAKOW, POLAND

Abstract

Poly-L-lactide (PLLA) is acknowledged biocompatible polyester. However, it possesses high crystallinity/brittleness/stiffness and requires long time for complete degradation. In the current study we present data on PLTMC, a copolymer of L-lactide and trimethylene carbonate (TMC). Poly(trimethylene carbonate) (PTMC) is characterised by good mechanical properties and rapid degradation rate and for this it might possess new desired features for medical applications. During the experiments, adhesion and activity of fibroblasts cultured on PLLA and PLTMC were studied and compared during two time points of 3 and 5 days. On day 3, the number of adherent fibroblasts was compromised when fibroblasts were cultured in the presence of PLTMC but the proper adherence was recovered by day 5. The same pattern was observed when we evaluated some activity parameters of fibroblasts. In particular, the release of proteins and nitric oxide was studied as the increased levels of the mediators might indicate unwanted inflammatory-like condition. Overall, the results suggest that the synthesized PLTMC initially shows unwanted effects on fibroblasts but with the time these effects are abolished. Therefore PLTMC seems to represent a new material that is non-cytotoxic and compatible with the living cells.

[Engineering of Biomaterials, 102, (2011), 7-10]

Introduction

Poly-L-lactide (PLLA) is one of the most promising biodegradable and absorbable aliphatic polyesters [1,2]. PLLA has been extensively used in biomedical applications, particularly those that demand good mechanical properties, biocompatibility, low toxicity and non-immunogenicity [3-7]. However, high crystallinity of PLLA, its brittleness, stiffness, long-time degradation and induction of local inflammatory reactions *in vivo*, consist the main obstacles to limit the applications of PLLA in tissue engineering [8-13]. The above properties of the biomaterial can be improved by copolymerization of L-lactide with other monomers, e.g. glycolide, ϵ -caprolactone, trimethylene carbonate (TMC) [14-16]. Among the bioresorbable polymers, poly(trimethylene carbonate) (PTMC) is of great interest, due to its elasticity combined with a slow degradation rate in aqueous solutions. Moreover, PTMC is characterized by rapid degradation *in vivo* via enzymatic decomposition without leading to the formation of acidic products, as in the case of PLLA [17,18].

Furthermore, the high molecular weight PTMCs yield relatively good mechanical properties [19]. Thus, PTMC is a preferable biodegradable polymer with good mechanical performance that possesses higher flexibility and evokes lower acidification of biological fluids than poly-L-lactide.

Therefore in this paper, biocompatibility of poly(L-lactide-co-trimethylene carbonate) and poly(L-lactide) was tested with the use of fibroblasts – one of the most numerous cell types in the body and good candidates for cytotoxicity/biocompatibility testing of different materials [20]. As model cells murine fibroblasts originating from the cell line L-929 were used.

Materials and Methods

Materials production and characterization

A copolymer of L-lactide and trimethylene carbonate (PLTMC, molar ratio of co-monomers 50:50; Mn = 68 kDa, d = 1.8) was kindly provided by Prof. P. Dobrzynski (Center of Polymer and Carbon Materials, Polish Academy of Sciences, Zabrze). Synthesis of PLTMC was performed with a low-toxic zirconium (IV) acetylacetonate as an initiator according to a method previously described in detail [21]. Poly-L-lactide (PLLA) with a viscosity-average molecular weight M_v of 410 kDa was bought from Purac (the Netherlands).

The PLLA and PLTMC foils were cast from 10% (w/v) polymer solution in methylene chloride (POCh, Gliwice, Poland) on glass Petri dishes, followed by air drying for 24 h and vacuum drying for the next 72 h. Then, the foils were rinsed with ultra high purity water (UHQ-water of the resistivity of 18.2 M Ω cm, produced by Purelab UHQ, Elga, UK) for 12 h. UHQ-water was exchanged 6 times. Afterwards, the foils were air and vacuum dried for 24 h and 72 h, respectively. The resulting foils had a thickness of 0.18 mm. For all experiments the bottom surface of the foils, e.g. contacting glass during preparation process was used.

The water contact angle was measured by sessile drop method by an automatic drop shape analysis system DSA 10 Mk2 (Kruss, Germany) with the use of UHQ-water. The surface topography and root-mean square roughness (R_{rms}) were evaluated by atomic force microscopy in contact mode (AFM Explorer, ThermoMicroscopes, Veeco, USA) in the scan areas of 100 μ m x 100 μ m. The results were presented as means \pm SD of ten (contact angle) and four (R_{rms} roughness) individual measurements for each sample.

Cell cultures

For cell culture studies the polymeric foils and control glass cover slips were washed in 70% ethanol, sterilized with UV irradiation (45 min for each side) and placed at the bottom of 24-well dishes (Nunc, Denmark).

The fibroblast cell line L-929 of mouse origin was used in the studies. The cells were cultured in 75-ml plastic bottles (Nun, Denmark) in DMEM culture medium enriched with glucose, L-Glutamine (PAA, Austria), 10% foetal bovine serum (PAA, Austria) and 5% antibiotic solution (Sigma-Aldrich, Germany) containing penicillin (10 UI/ml) and streptomycin (10 mg/ml). The cells were cultured in the incubator (Nuaire, USA) at 37°C and 5% of CO₂.

Every 2-3 days, when the cells were forming high confluence monolayers, the cell cultures were passaged by trypsinization (0.25% solution of trypsin; Sigma-Aldrich, Germany). The cells that were harvested after 7 to 10 passages were used in the studies. They were counted in Burkert's haemocytometer and diluted to 3x10⁴ cell/ml, and thereafter placed in the wells of 24-well culture dishes (Nunc, Denmark) containing discs of tested biomaterials or rounded cover glasses (controls). In such conditions the cells were cultured for 3 or 5 days.

Cell adherence studies

The ability of the cells to adhere to glass or polymeric surfaces was tested using the crystal violet test (CV). The cells adhering to the foils or glass were fixed with 2% paraformaldehyde for 1 h, and then stained with crystal violet (CV; 0.5% in 20% methanol, 5 min). After that time the foils and glass coverslips were washed with water and transferred to a new 24-well culture plate. After drying, the absorbed dye was extracted by addition of 1 ml of 100% methanol (POCh, Gliwice) to every well. After that the optical density (O.D.) was measured at 570 nm with the Expert Plus spectrophotometer (Asys Hitach, Austria). Since the polymers absorb some crystal violet, additional controls were run. These were containing biomaterials and cell-free medium only.

Nitric oxide (NO) studies

Fibroblast activity was evaluated by the Griess method that allows for measurement of nitric oxide (NO) concentration in supernatants collected from cell cultures. First 100 μ l of the supernatant was added to the wells of a 96-well plate and then 100 μ l of a mixture of Griess reagent A and B (1:1) was added (A: 1% sulfamylamide in 5% H_3PO_4 , B: 0.1% naftylenediamine in H_2O ; Sigma-Aldrich, Germany). After 5-min incubation the optical density was measured at 570 nm with spectrophotometr Expert Plus (Asys Hitach, Austria).

Protein production

Protein concentration in the supernatants collected from cell cultures was measured by the colorimetric BCA method. A mixture of copper (II) sulfate solution (CS, Sigma, Germany) and bicinchoninic acid solution (BCA; Sigma, Germany) in ratio 1:50 was firstly prepared. Subsequently, 10 μ l of each tested sample was transferred to the wells of a 96-well plate and then 200 μ l of the CS/BCA mixture was added. The plates were incubated for 30 min in the dark. After that time the optical density was measured at 570 nm with Expert Plus spectrophotometer (Asys Hitach, Austria).

Statistical analysis

ANOVA followed by a *post-hoc* T-Tukey test was used for statistical analysis; $p < 0.05$ was considered as statistically significant. All values are reported as means \pm SE.

Results and discussion

Properties of polymer foils

It is widely accepted that surface chemistry and surface topography are regarded as important parameters which influence biological properties (e.g. cell adhesion, proliferation, activation and secretion) of artificial materials and as results have the impact on their biocompatibility. To this end hydrophobic/hydrophilic properties and topography/roughness of polymer materials used in this study were characterised. Water contact angle and R_{rms} roughness values of the studied materials are gathered in TABLE 1. PLLA and PLTMC are relatively hydrophobic and exhibit similar, high water contact angles values of about 80 degrees, and any statistical differences were found between them. PLLA surface was more rough and textured with well developed crystalline spherulites consisting on lamellae (FIG. 1A). On the contrary, the surface of PLTMC was smooth, flat and less textured (FIG. 1B). R_{rms} values of PLLA were significantly higher than those of PLTMC.

TABLE 1. Water contact angle and RRMS roughness of polymeric materials; means \pm SD.

| Material | Water contact angle (degree) | R_{rms} (nm) |
|----------|------------------------------|----------------|
| PLLA | 78.3 ± 2.6 | 160 ± 24 |
| PLTMC | 80.5 ± 1.3 | 48 ± 18 |

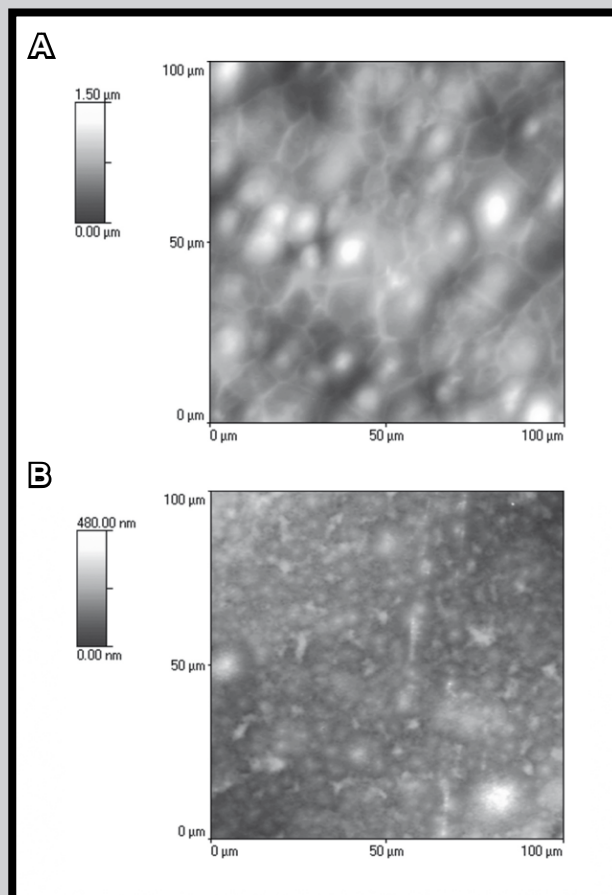


FIG. 1. AFM Surface topography of PLLA (A) and PLTMC (B).

Cell cultures

L-929 fibroblast cell line is frequently used to test cytotoxicity and it is one of the recommended cell lines for biocompatibility testing due to its optimal sensitivity and easiness of culture [20]. For the determination of biocompatibility of the PLTMC, in comparison to PLLA and glass, the mouse fibroblasts L-929 were tested for their adhesion to the materials as well as their activation state.

The cell adhesion is an important step in a wide variety of biological processes. It depends on the biocompatibility of synthetic implant materials and it plays a key-role in tissue and organ formation and in generation of traction for migration of cells [22]. In our studies we tested fibroblasts cultured on PLLA, PLTMC and control glass for 3 and 5 days (FIG. 2). On day 3, the number of adherent fibroblasts was comparable to the control in the case of the PLLA, but the presence of PLTMC decreased the cell adherence (FIG. 2A). On day 5, the number of adherent fibroblasts on the PLLA was even higher than that on the control and, importantly, it was not altered on the PLTMC (FIG. 2B). This shows that although at first PLTMC had an unfavourable effect on fibroblast adherence this has changed with time suggesting its proper biocompatibility.

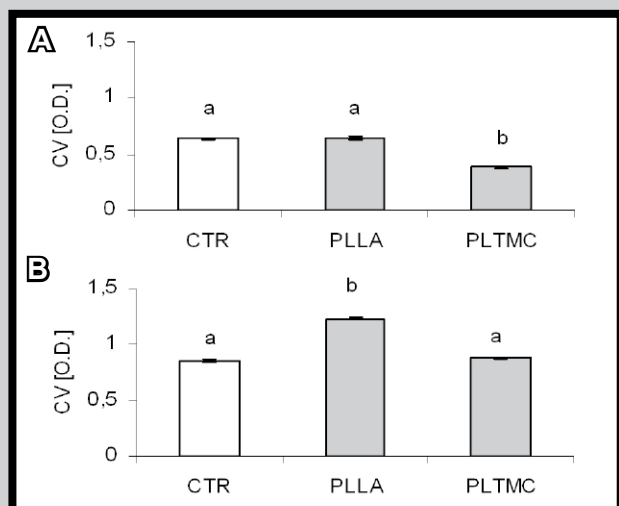


FIG. 2. Ability of murine fibroblasts L-929 to adhere to control/polymeric surfaces after 3 (A) and 5 (B) days of culture on either control glass or polymers PLLA and PLTMC. O.D. - optical density measured at 570 nm. The results are presented as means \pm SE. Different letters (e.g. a vs. b) indicate statistically significant differences between the groups according to ANOVA.

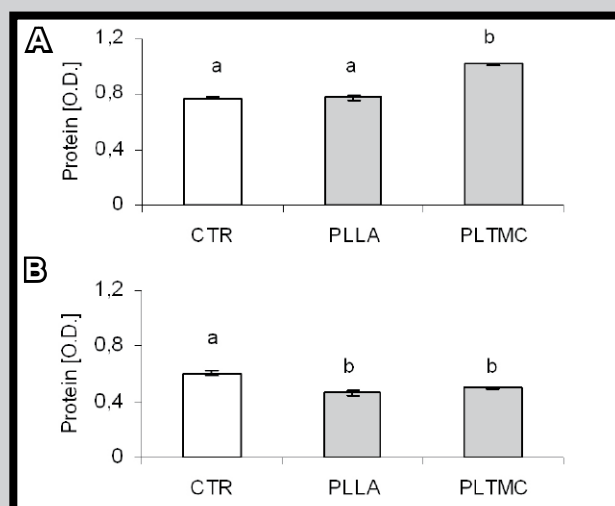


FIG. 4. Total protein content in supernatants collected from murine fibroblast L929 cultures after 3 (A) and 5 (B) days on either control glasses or polymers PLLA and PLTMC. O.D. - optical density measured at 570 nm. The results are presented as means \pm SE. Different letters (e.g. a vs. b) indicate statistically significant differences between the groups according to ANOVA.

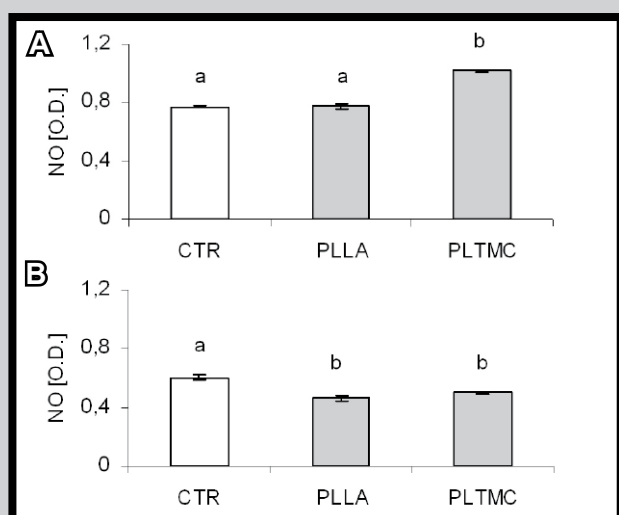


FIG. 3. Nitric oxide (NO) levels in supernatants collected from murine fibroblast L-929 cultures after 3 (A) and 5 (B) days on either control glasses or polymers PLLA and PLTMC. O.D. - optical density measured at 570 nm. The results are presented as means \pm SE. Different letters (e.g. a vs. b) indicate statistically significant differences between the groups according to ANOVA.

The attachment of mouse fibroblast NIH/3T3 to the PLLA and PLTMC was also studied by *Ji and co-workers* [15]. Their results showed that after 24 h incubation the fibroblasts spread much better and had better size/morphology on PLTM than PLLA. Moreover, the prolonged (4-5 days) culture of the cells significantly increased cell proliferation when cultured on PLTMC, but not on PLLA, in comparison to the control glass [15]. Therefore their results revealed similar pattern as observed in our studies, however, this should be pointed out that *Ji and co-workers* [15] used another ratio of L-lactide and TMC (85:15) than was used in our analyses (50:50) and they tested another fibroblast cell line (NIH/3T3 vs. L-929, respectively).

On the other hand, *Yang et al.* [14] tested adherence of multiple homo- and heteropolymers on platelet adhesion. Low degree of activation with few adhered platelets indicates good anticoagulant properties of the polymer and the haemolytic ratio (HR) below 5% is acceptable for medical application. In the case of PLTMC (50:50) the HR value was 1.6% and it was the lowest among the other tested heteropolymers [14]. In general, whenever PLLA was modified by synthesis of heteropolymers with various, sometimes very different, polymers the resulting heteropolymer had improved cell adherence and/or cell proliferation properties. For example, *Casarano and co-workers* [23] documented enhanced cell adhesion and proliferation rate when 3T3-L1 fibroblasts were cultured in presence of heteropolymer of PLLA and poly(isosorbide succinate-*b*-L-lactide).

Interactions between materials and cells may influence the secretory activity. Nitric oxide (NO), a short-lived radical is an important immune mediator with profound cytotoxic reaction towards surrounding cells and tissues [24]. Consequently, nitric oxide serves as a good indicator of inflammation and should be monitored e.g. during the wound healing process [25]. Our results demonstrated that on day 3 production of nitric oxide by fibroblasts cultured on PLTMC was significantly increased in comparison to the control glass and PLLA (FIG. 3A). However, after 5-day incubation fibroblasts cultured on either PLLA or PLTMC polymers produced significantly less NO than the control fibroblasts (FIG. 3B). Therefore once again we observed that the initially undesired reaction was normalized with time.

The increased synthesis of NO might indicate that also other inflammatory mediators are being generated. For this we evaluated total levels of released proteins in the culture supernatants. As expected, we detected that on day 5 secretion of proteins in the presence of both PLLA and PLTMC was decreased in comparison to the control glass (FIG. 4B) while at first, on day 3, it was increased in the presence of PLTMC (FIG. 4A).

In the current preliminary study we measured the basic parameters evaluating cell biocompatibility such as cell ability to adhere to the tested polymers (also indirectly indicative of cell viability) and their activity estimated by ratio of released proteins, and potentially cytotoxic/inflammatory NO. Overall, the results suggest that the PLTMC (50:50) initially shows unwanted effects on fibroblasts but with time (within only two days) these effects are abolished. Therefore PLTMC seems to be non-cytotoxic and compatible with the living cells.

Our further work will concentrate on detailed studies of PLTMC effects on fibroblasts and other cell types as well as analyses of production of particular biological mediators.

Acknowledgements

This study was supported by the research grant No. 215/KF/2007 from the Academy of Physical Education, Krakow (Poland), and from the Polish Budget Funds for Scientific Research within the years 2009-2012, as a research project N° N507280736.

References

- [1] J.C. Middleton, A.J. Tipton. Synthetic biodegradable polymers as orthopedic devices. *Biomaterials* 21, 2000: 2335-2346.
- [2] Y. Tokiwa, A. Jarerat. Biodegradation of poly(L-lactide). *Biotechnol Lett* 26, 2004:771-777.
- [3] H. Cai, V. Dave, R.A. Gross, S.P. McCarthy. Effect of physical aging, crystallinity and orientation on the enzymatic degradation of poly(lactid acid). *J Polym. Sci B: Polym Phys* 34, 1996: 2701-8.
- [4] N. Ogata, G. Jimenez, H. Kawai, T. Ogihara. Structure and thermal/mechanical properties of poly(9L-lactide)-clay blend. *J Polym Phys* 35, 1997: 389-96.
- [5] N. Grabow, M. Schlun, K. Sternberg, N. Hakansson, S. Kramer, K.P. Schmitz. Mechanical properties of laser cut poly(L-lactide)micro-specimens: implications for stent design, manufacture, and sterilization *Trans. ASME. Biomach Eng* 127, 2005: 25-31.
- [6] Y.S. Wong, S.S. Venkatraman. Recovery as a measure of oriented crystalline structure in poly(L-lactide) used as shape memory polymer. *Acta Mater*, 58, 2010: 49-58
- [7] K.A. Athanasiou, G.G. Niederauer, C.M. Agrawal. Sterilization, toxicity, biocompatibility and clinical applications of polylactic acid/polyglycolic acid copolymers. *Biomaterials*, 17, 1996: 93-102
- [8] L.S. Nair, C.T. Laurencin. Biodegradable polymers as biomaterials. *Prog Polym Sci* 32, 2007: 762-98.
- [9] D.A. Garlota. A literature review of poly(lactid acid). *J Polym Environ* 9, 2001: 63-84.
- [10] R.M. Rasal, D.E. Hirt. Toughness decrease of PLA-PHBHx blend films upon surface-confined photopolymerization. *J Biomed Mater Res Part A* 88A, 2008: 1079-86.
- [11] M. Hiljanem-Vainio, P. Varpomaa, J. Seppala, P. Tormala. Modification of poly(L-lactides) by blending: mechanical and hydrolytic behavior. *Macromol Chem Phys* 197, 1996: 1503-23.
- [12] M. Nakagawa, F. Teraoka, S. Fujimoto, Y. Hamada, H. Kibayashi, J. Takahashi. Improvement of cell adhesion on poly(L-lactide) by atmospheric plasma treatment. *J Biomater Res A* 77, 2006: 112-8.
- [13] H. Yanagida, M. Okada, M. Maruda, M. Ueki, I. Narama, S. Kitao, Y. Koyama, T. Furuzono, K. Takakuda. Cell adhesion and tissue response to hydroxyapatite nanocrystal-coated poly(L-lactid acid) fabric. *J Biosci Bioeng* 108, 2009: 235-43.
- [14] J. Yang, F. Liu, S. Tu, Y. Chen, X. Luo, Z. Lu, J. Wie, S. Li. Haemo- and cytocompatibility of bioresorbable homo- and copolymers prepared from 1,3-trimethylene carbonate, lactides, and ϵ -caprolactone. *J Biomed Mater Res A* 94, 2010a: 396-407.
- [15] L.J. Ji, K.L. Lai, B. He, G. Wang, L.Q. Song, Y. Wu, Z.W. Gu. Study on poly(L-lactide-co-trimethylene carbonate): synthesis and cell compatibility of electrospun film. *Biomed Mater* 5, 2010: 1-8.
- [16] J. Yang, F. Liu, L. Yang, S. Li. Hydrolytic and enzymatic degradation of poly(trimethylene carbonate-co-D,L-lactide) random copolymers with shape memory behavior. *Eur Polym J* 46, 2010b: 783-791.
- [17] Z. Zhang, R. Kuijter, S.K. Bulstra, D.W. Grijpma, J. Feijen. The in vivo and in vitro degradation behavior of poly(trimethylene carbonate). *Biomaterials* 27, 2006: 1741-8.
- [18] K.J. Zhu, R.W. Hendren, K. Jansen, C.G. Pitt. Synthesis, properties, and biodegradation of poly(1,3-trimethylene carbonate). *Macromolecules* 24, 1991: 1736-40.
- [19] A.P. Pego, D.W. Grijpma, J. Feijen. Enhanced mechanical properties of 1,3-trimethylene carbonate polymers and networks. *Polymer* 44, 2003:6495-504.
- [20] A. Neumann, T. Reske, M. Held, K. Jahnke. Comparative investigation of the biocompatibility of various silicon nitride ceramic qualities in vitro. *J Mater Sci: Mat In Med* 14, 2004: 1135-1140.
- [21] P. Dobrzynski, J. Kasprczyk. Synthesis of biodegradable copolymers with low-toxicity zirconium compounds. V. Multiblock and random copolymers of L-lactide with trimethylene carbonate obtained in copolymerizations initiated with zirconium(IV) acetylacetonate. *J Polym Sci Part A* 44, 2006: 3184-3201.
- [22] K. Kwon, K.D. Park, S.W. Choi, S.H. Lee, E.B. Lee, J.S. Na, S.H. Kim, Y.H. Kim. Fibroblasts culture on surface-modified poly(glycolide-co-caprolactone) scaffolds for soft tissue regeneration. *J Biomater Sci Polymer Edn* 10, 2001: 1147-1160.
- [23] R. Casarano, R. Bentini, V.B. Bueno, T. Lacovella, F.B.F. Monteiro, F.A.S. Iha, A. Campa, D.F.S. Petri, M. Jaffe, L.H. Catalani. Enhanced fibroblast adhesion and proliferation on electrospun fibers obtained from poly(isosorbide succinate-b-L-lactide) block copolymers. *Polymer* 50, 2009: 6218-6227.
- [24] P. Pacher, J.S. Beckman, L. Liaudet. Nitric oxide and peroxynitrate in health and disease. *Physiol Rev* 87, 2007: 315-424.
- [25] K. Yamasaki, H. Edington, C. McClosky, E. Tzeng, A. Lizonova, I. Kovacs, D. Steed and T. Billiar. *J Clin Invest* 101, 1998: 967.

CHEMICAL MODIFICATION OF POLY ϵ -CAPROLACTONE WITH WOLLASTONITE AND ITS INFLUENCE ON BIOLOGICAL PROPERTIES OF OSTEOBLAST LIKE-CELLS MG-63

ANNA ŚCISŁOWSKA-CZARNECKA¹, ELŻBIETA MENASZEK^{2,4},
ELŻBIETA KOŁACZKOWSKA³, MARTA BŁĄŻEWICZ⁴,
JOANNA PODPORSKA⁴

¹ DEPARTMENT OF ANATOMY,
ACADEMY OF PHYSICAL EDUCATION, KRAKÓW, POLAND

² DEPARTMENT OF CYTOBIOLOGY,
JAGIELLONIAN UNIVERSITY, KRAKÓW, POLAND

³ DEPARTMENT OF EVOLUTIONARY IMMUNOBIOLOGY,
JAGIELLONIAN UNIVERSITY, KRAKÓW, POLAND

⁴ DEPARTMENT OF BIOMATERIALS,
AGH UNIVERSITY OF SCIENCE AND TECHNOLOGY,
KRAKÓW, POLAND

Abstract

PCL (poly- ϵ -caprolactone) is a biocompatible and biodegradable polymer of aliphatic polyester group. However, PCL does not effectively bind to the bone in contrast to bioactive inorganic compounds such as wollastonite. For this wollastonite (WS) is regarded as a potential bioactive material for bone tissue engineering although its main drawback is brittleness. Therefore we synthesized polymer nanocomposite materials composed of poly- ϵ -caprolactone and wollastonite (PCL/wollastonite) containing either 0.5% or 5% of the latter modifying filler. And we aimed to verify biological properties of the nanocomposite PCL/WS materials, in comparison to the pure PCL, on cultures of osteoblast-like cells MG-63. The study revealed that the adherence of the osteoblast-like cells to the tested materials was enhanced by the PCL modification (PCL/5WS > PCL/0.5WS > PCL) while cell viability/proliferation was not altered. Furthermore, the activity of alkaline phosphatase indicative of osteoblast differentiation (maturation) was enhanced when the cells were cultured with either PCL/5WS or PCL/0.5WS. Overall, our results indicate that PCL-modified wollastonite improves biological properties of the basic biomaterial suggesting its potential usefulness/application for the bone tissue regeneration.

Keywords: polycaprolactone, wollastonite, osteoblast-like MG-63 cells, cell adhesion, viability, proliferation, alkaline phosphatase

[*Engineering of Biomaterials*, 102, (2011), 11-14]

Introduction

Biodegradable polymers are widely used in bone regeneration. PCL (poly- ϵ -caprolactone) is a biodegradable polymer of aliphatic polyester group. Due to its semi-crystalline nature and hydrophobicity, degradation of PCL is remarkably slow (years) since the close packed macromolecular arrays retard fluid ingress in the bulk [1]. PCL is highly compatible with osteoblasts and, hence, it may be suitable for long-term implant applications [2]. PCL has attracted much interest

because of its cost-efficiency, high toughness, and processability resulting from its relatively low melting temperature. Poly- ϵ -caprolactone is a non-toxic product, having good ability to mix and good mechanical compatibility with bioactive materials [3].

Tissue engineering offers a promising new approach for bone repair. Significant characteristics of bioactive materials are connected with their ability to bind with living bone through formation of an apatite interface layer. Moreover, various types of biomaterials containing CaSiO_3 , such as bioactive glasses, glass-ceramics, and wollastonite are regarded as potential bioactive materials for bone tissue regeneration due to their osseointegration properties [4-6]. Some studies have shown that wollastonite has excellent bioactivity and is a potential candidate of new biomaterials for tissue repair [7]. However, the extensive use of wollastonite is limited by its dissolution and high degradation rate leading to a high pH value in the surrounding environment [8,9] which can disadvantage cell growth thereby affecting their osseointegration ability [10].

Yet, there exist no pure polymers that can effectively bind to the bone *in vivo*, thus the composites of biodegradable polymers with bioactive inorganic phases are still a promising approach. Accordingly, combination of PCL with bioactive inorganic materials could bring out the advantages of both materials. Therefore, the aim of this study was to investigate effects of polymer nanocomposite material composed of poly- ϵ -caprolactone/wollastonite (PCL/WS) on biological properties of osteoblasts-like cells MG-63.

Materials and methods

Surface modification

Poly- ϵ -caprolactone (PCL) was purchased from Sigma-Aldrich and it was used as a matrix raw-material for nanocomposites. PCL characteristic were as follows: molecular mass, M_n 80,000; melting temp. 60°C; polydispersion, M_w/M_n < 2; the degree of crystallinity determined by DSC, 42.2%. Wollastonite nanopowder was used as a modifier of PCL. It was synthesised at the Department of Biomaterials, AGH University of Science and Technology (Kraków, Poland), based on poly-methyloxosilane resin Lukosil 901 (Lucebni Zavody, Kolin, Czech Republic) as a precursor. Silica (SiO_2) and calcium hydroxide $\text{Ca}(\text{OH})_2$ were applied as inorganic additives. The resin was thermally cross-linked, milled and then mixed with inorganic additives using the weight ratio 65:35 (10SiO_2 , $25\text{Ca}(\text{OH})_2$). The pellets were formed from powder mixture by uniaxial pressing and the prepared material was subjected to pyrolysis in neutral atmosphere at the temperature of 1000°C during 24 h, with heating rate of 0.7°C/min. Wollastonite (WS) ceramic made in this way contained silica oxycarbide (about 10 wt %), being formed during the pyrolysis of the resin. Thus obtained ceramic product was then milled in an attritor grinder for 12 h. In order to define the average grain size and the grain size distribution, the Nanosizer-ZS Malvern Instruments were used, having the ability to measure the size of particles in the range from 0.6 nm to 6 mm.

The polymer matrix nanocomposite samples were prepared in the form of foils of 0.2 mm thick. Dichloromethane was applied as a solvent of PCL matrix material to which wollastonite powder was added and then the suspensions were homogenized with use of an ultrasonic homogenizer, making the suspension uniform and breaking down powder soft agglomerates [11-13]. Nanocomposite samples were prepared, containing the following amounts of modifying filler (by volume): PCL/0.5% and PCL/5%. Samples without wollastonite content were prepared as reference materials.

Cell culture

For cell culture studies the resorbable polymers (PCL/WS) were washed in 70% ethanol and sterilized with UV irradiation (45 min for each side). The osteoblast-like cells MG-63 were routinely grown in 75 ml flasks in Dulbecco's Modified Eagle Medium with glucose and L-Glutamine (PAA, Austria), 10% foetal bovine serum (PAA, Austria), 100 U/mL penicillin, and 100 µg/mL streptomycin (Sigma, Germany) in a 5% CO₂ and 95% air atmosphere at 37°C. A flask of cells was brought into suspension after incubating for 5 min with 0.5% trypsin plus EDTA (PAA, Austria). Following trypsinization, the cells were washed by centrifugation at 400 g for 5 min to form a pellet that was resuspended in fresh supplemented medium to a concentration of 3×10^4 cells/ml. Next, 1 ml of cell suspension was added to each well of 24-well plates (Nunc, Denmark) containing sterile nanocomposite samples. Samples without wollastonite (pure PCL) served as a control. Cultures were performed for 3 or 7 days at 37°C in a 5% CO₂ and 95% air atmosphere.

Biological properties

At the selected time points (3 or 7 days), supernatants from the above cells cultured on biomaterials were collected and frozen for osteoblast activity evaluation.

Afterwards, the cells were stained for 2 min. with 0.01% acridine orange in PBS, washed with PBS, and the cell cultures were observed and photographed under the fluorescence microscope for evaluation of their morphology and attachment to the studied biomaterials.

Estimation of adherent cell mass was achieved by crystal violet staining/extraction (CV test). Cells cultured on studied materials were washed twice with PBS (phosphate buffered saline), fixed in 2% paraformaldehyde for 1 h at 21°C and stained with 0.5% crystal violet in 20% methanol for 5 min. Then the cells were washed with tap water, and dried in air. The adsorbed stain was extracted by addition of 1 ml of 100% methanol (POCH, Gliwice, Poland) and optical density was measured with an Expert Plus spectrophotometer (Asys Hitech, Eugendorf, Austria) at 570 nm.

The viability of cells was estimated by the MTT assay. Briefly, a 100 µl of 5 mg/ml MTT (3-[4,5-dimethyl-thiazol-2-yl]-2,5-diphenyltetrazolium bromide, Sigma-Aldrich, Germany) water solution was added to each well. After 1 h incubation in the dark at 37°C the reaction was stopped by pouring 1 ml of isopropanol containing 3% of HCl (POCH, Gliwice, Poland) and the optical density of formazan was determined at 570 nm with the Expert Plus spectrophotometer.

Protein concentration in the supernatants was measured by the colorimetric BCA method. A mixture of copper (II) sulphate solution (CS, Sigma-Aldrich, Germany) and bicinchoninic acid solution (BCA; Sigma, Germany) in ratio 1:50 was firstly prepared. Subsequently, 10 µl of each tested sample was transferred to wells of a 96-well plate and then 200 µl/well of the CS/BCA mixture was added. The plates were incubated for 30 minutes in the dark. The optical density was measured at 570 nm with the Expert Plus spectrophotometer.

For assessment of alkaline phosphatase (ALP), the production of p-nitrophenol in the presence of ALP was measured by a bone-specific immunoassay (Metra BAP EIA kit; Quidel, San Diego, USA) according to the manufacturer's instructions.

Statistical analysis

The results were reported as mean values \pm the standard error (SEM). Statistical analyses were performed using the T-Tukey's test. The statistical significance of differences was set at $p < 0.05$.

Results and discussion

In this study, we evaluated biological properties of pure PCL and its modifications i.e. nanocomposites with wollastonite (PCL/WS) using the osteoblast-like MG-6 cell culture system, which has been frequently used for elucidating the responses of bone cells to biomaterials [14]. A proper cell attachment belongs to the first phase of cell/material interactions and the quality of this first phase will influence the cell capacity to grow and proliferate as well as the cell morphology, proliferation and viability upon contact with the implant material. In the present study the relative number of cells adhering to different materials was assessed using crystal violet (CV) assay because cell absorbance of CV serves as an indicator of the relative number of cells on the materials. The results of the cell attachment studies revealed that osteoblast adherence to the materials was improved by one of the PCL modifications (PCL/5%WS) already on day 3 of the experiment. However, the long term (7-day) incubation with either wollastonite modification of PCL significantly improved osteoblast ability to adhere in comparison to the unmodified PCL (FIG. 1). Fluorescent microscopy showed the morphological features of osteoblast-like cells cultured on the PCL, PCL/0.5WS and PCL/5WS (as showed for 7 days on the FIG. 2). Apparently significantly more cells were present when the cells were cultured on the wollastonite nanocomposites of PCL (PCL/5WS > PCL/0.5WS) then on the pure PCL (FIG. 2). This is in line with our data from the CV studies and with reports of other groups. In particular, Ni and co-workers [15,5] investigated bioactive porous CaSiO₃ scaffolds and examined their effects on adherence and proliferation of the osteoblast-like cells. On day 7 of incubation the two parameters were improved as compared to the control [5]. A similar phenomenon was observed by Wei and co-workers [16]. The osteoblast-like cells adhered better to the mesoporous wollastonite/PCL composite scaffolds (m-WSP/PCL) than to that of PCL or tissue culture plate.

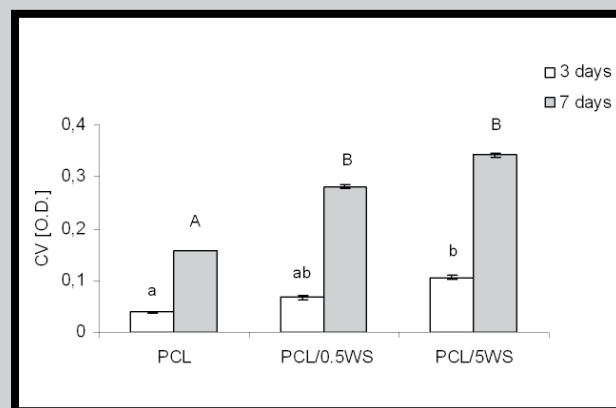


FIG. 1. The adherence of osteoblast-like MG-63 cells to PCL (poly ϵ -caprolactone), and modified PCL [poly ϵ -caprolactone/0.5% wollastonite (PCL/0.5WS) and poly ϵ -caprolactone/5% wollastonite (PCL/5WS)] at 3 and 7 days of culture. O.D. - the optical density measured at 570 nm. The results are presented as means \pm SE. Different letters (e.g. a vs. b or A vs. B) indicate values significantly different when tested against PCL by means of the T-Tukey's test ($p < 0.05$).

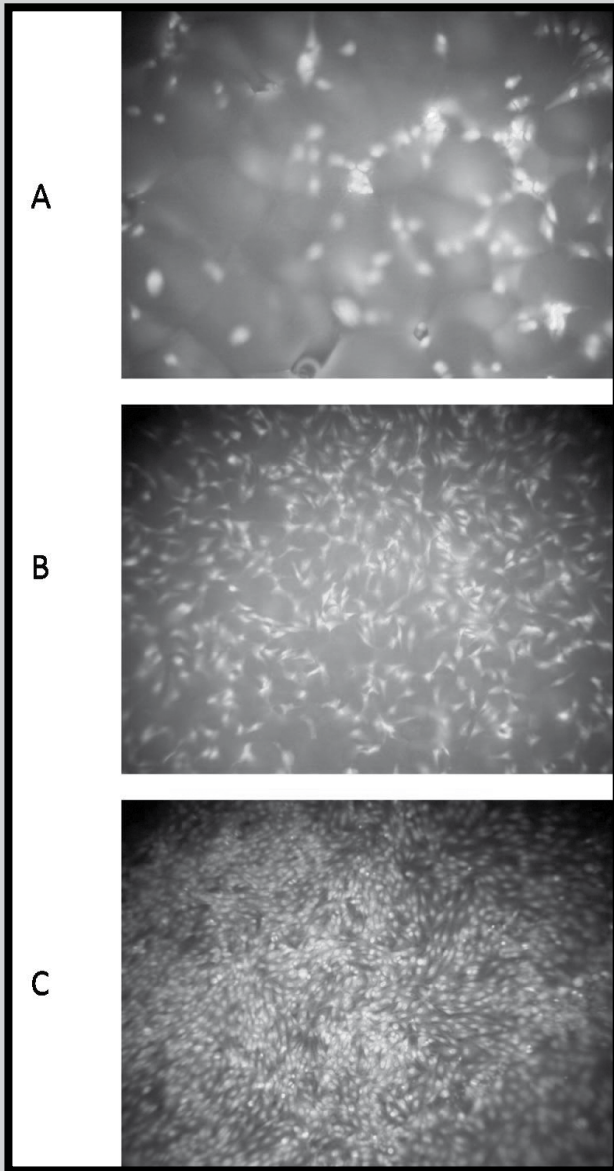


FIG. 2. Morphology of osteoblasts-like cells (MG-63) grown on a control material PCL and on modified PCL nanocomposites [poly ϵ -caprolactone/0.5% wollastonite (PCL/0.5WS) and poly ϵ -caprolactone/5% wollastonite (PCL/5WS)] analyzed by fluorescence microscopy after 7-day incubation. (A) PCL, (B) PCL/0.5WS, and (C) PCL/5WS.

It is known that the cellular responses to a given material, such as adhesion, proliferation and differentiation depend not only on its physical status but also on its chemical composition which is relevant to the level of ions released from the material and consequent cell-material interactions. Consequently, it was shown that solution containing high Si concentrations is mitogenic for bone cells [17]. Moreover, Xynos [18] reported that ionic products (Si and Ca) of bioactive glass dissolution could stimulate osteoblast proliferation. In the current studies we evaluated viability/proliferation of the osteoblast-like cells by the MTT test (FIG. 3). The viability/proliferation of MG-63 cells was not altered between the polymer nanocomposite samples and the PCL control. Therefore the obtained results indicate that the developed PCL/wollastonite nanocomposites are not cytotoxic.

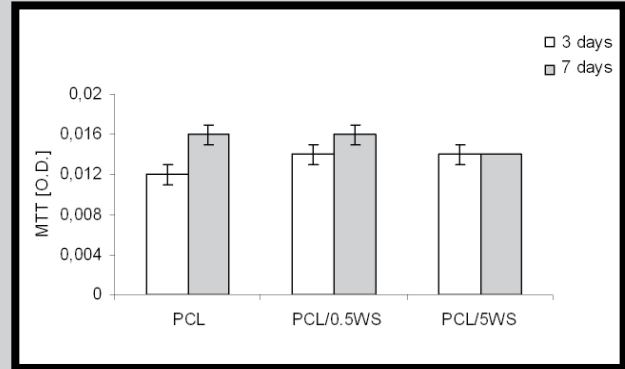


FIG. 3. The viability/proliferation of osteoblast-like MG-63 cells on PCL (poly ϵ -caprolactone), and modified PCL [poly ϵ -caprolactone/0.5% wollastonite (PCL/0.5WS) and poly ϵ -caprolactone/5% wollastonite (PCL/5WS)] at 3 and 7 days of culture. O.D. - the optical density measured at 570 nm. The results are presented as means \pm SE.

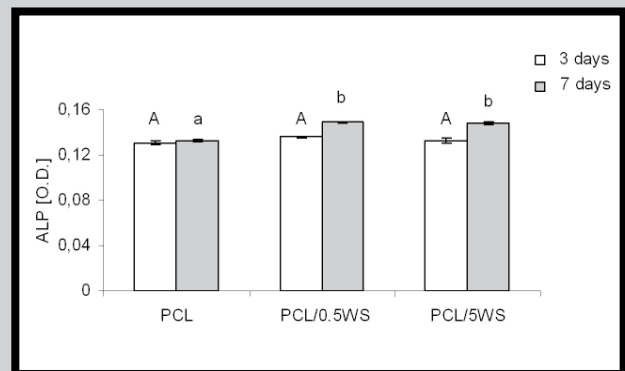


FIG. 4. Alkaline phosphate (ALP) activity of osteoblast-like MG-63 cultured with the PCL (poly ϵ -caprolactone) and modified PCL [poly ϵ -caprolactone/0.5% wollastonite (PCL/0.5WS) and poly ϵ -caprolactone/5% wollastonite (PCL/5WS)]. ALP content was measured in supernatants collected from osteoblasts cultured in the presence of the polymers for either 3 or 7 days. The results are presented as means \pm SE. Different letters (e.g. a vs. b or A vs. B) indicate values significantly different when tested against the control by means of the T-Tukey's test ($p < 0.05$).

Additionally, the lack of differences in proliferation rate might indicate that the cells have been translated to differentiation rather than division [19]. This was further confirmed by detection of higher levels of active alkaline phosphatase in supernatants of the cells cultured with PCL/0.5WS and PCL/5WS than PCL. This implies upregulated osteoblastic differentiation in the presence of wollastonite. Moreover, alkaline phosphatase ALP activity is recognized as an early marker for the functionality and activity of osteoblasts in *in vitro* experiments [20]. In particular, we detected that on day 3, the ALP activity observed in the supernatants of the cells cultured on both polymer composites (PCL/0.5WS and PCL/5WS) was comparable to the control PCL, but on day 7 the ALP activity was higher in the case of the nanocomposites than in the PCL cultures (FIG. 4). Similar effects have reported by Ni and co-workers when they studied effects of porous CaSiO_3 on osteoblast-like cells [15,5].

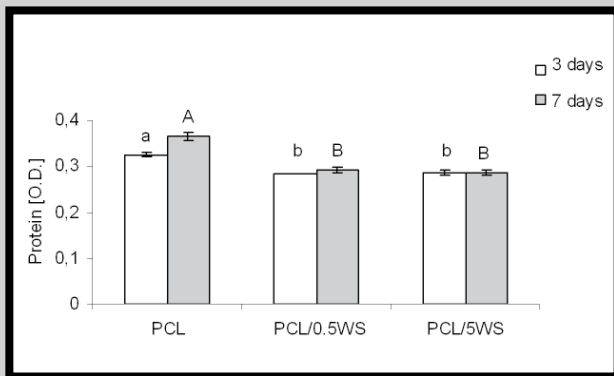


FIG. 5. Production/release of proteins by osteoblast-like MG-63 cells in the presence of the tested polymer samples. The cells were incubated with the PCL (poly ϵ -caprolactone) and modified PCL [poly ϵ -caprolactone/0.5% wollastonite (PCL/0.5WS) and poly ϵ -caprolactone/5% wollastonite (PCL/5WS)]. The total protein content was measured in supernatants collected from osteoblast cultured in the presence of the polymers for either 3 or 7 days. The results are presented as means \pm SE. Different letters (e.g. a vs. b or A vs. B) indicate values significantly different when tested against the control by means of the T-Tukey's test ($p < 0.05$).

Morphology and chemistry of the substrate/material might lead to new gene transcription and subsequently new protein synthesis [21]. For this we evaluated total levels of proteins released by the tested cells. On day 3 and 7 osteoblasts co-cultured with polymer nanocomposite samples PCL/0.5WS and PCL/5WS released less proteins than the cells cultured on the control PCL (FIG. 5). This might imply that the osteoblast-like cells do not become (over) activated by the nanocomposites as they do not increase the release of mediators/factors. In turn they differentiate and possibly mature into osteocytes forming bones.

Nanocomposites made of resorbable polymers (PCL) and ceramic nanoparticles (wollastonite) may become good alternative materials for growing bone tissue cells, in view of their superior mechanical and bioactive properties compared to conventional materials as well as desired biological properties. The above results suggest that poly- ϵ -caprolactone/wollastonite nanocomposites may be potential candidates for preparation of bioactive bone substitutes.

Conclusion

In conclusion, the results of this study demonstrate *in vitro* cell compatibility of the polymer matrix nanocomposite materials PCL/0.5WS and PCL/5WS and suggest their potential applications for bone tissue engineering.

References

- [1] D. Puppi, F. Chiellini, A.M. Piras, E. Chiellini. Polymeric materials for bone and cartilage repair. *Prog in Polym Sci* 35, 2010: 403-440.
- [2] J.F. Mano, R.A. Sousa, L.F. Boesel, N.M. Neves, R.L. Reis. Bioinert biodegradable and injectable matrix composites for hard tissue replacement: state of the art and recent developments. *Comp Sci Technol* 64, 2004: 789-817.
- [3] L. Shor, S. Guceri, X. Wen, M. Gandhi, W. Sun. Fabrication of three-dimensional polycaprolactone/hydroxyapatite tissue scaffolds and osteoblast-scaffolds interactions *in vitro*. *Biomaterials* 28, 2007: 5291-5297.
- [4] W. Xue, X. Liu, X.B. Zheng, C. Ding. *In vivo* evaluation plasma-sprayed wollastonite coating. *Biomaterials* 26, 2005: 3455-3460.
- [5] S. Ni, J. Chang, L. Chou, W. Zhai. Comparison of osteoblast-like cell responses to calcium silicate and tricalcium phosphate ceramics *in vitro*. *J Biomed Mater Res B Appl Biomater* 80, 2007: 174-183.
- [6] J. In-Kook, S. Ju-Ha, C. Won-Yong, K. Yong-Hang, K. Hyoun-Ee, K. Hae-Won. Porous hydroxyapatite scaffold coated with bioactive apatite-wollastonite glass-ceramics. *J Am Ceram Soc* 90, 2007: 2703-2708.
- [7] N. Sahai, A. Michel. Cyclic silicate active site an stereochemical match for apatite nucleation on pseudowollastonite bioceramic-bone interfaces. *Biomaterials* 26, 2005: 5763-5770.
- [8] P. Siriphannon, Y. Kameshima, A. Yasumori, K. Okada, S. Hayashi. Formation of hydroxyapatite on CaSiO_3 powders in simulated body fluid. *J Eur Ceram Soc* 22, 2002: 511-520.
- [9] Y. Imori, Y. Kameshima, K. Okada, S. Hayashi. Comparative study of apatite formation on CaSiO_3 ceramics in stimulated body fluids with different carbonate concentrations. *J Mater Sci Mater Med* 16, 2005: 73-79.
- [10] A. El-Ghannam, P. Ducheyne, I.M. Shapiro. Formation of surface reaction products on bioactive glass and their effects on the expression of the osteoblastic phenotype and the deposition of mineralized extracellular matrix. *Biomaterials* 18, 1997: 295-303.

- [11] X. Liu, C. Ding. Phase compositions and microstructure of plasma-sprayed wollastonite coating. *Surf Coat Technol* 141, 2001: 269-274.
- [12] W. Xue, C. Ding. Plasma sprayed wollastonite/ TiO_2 composite coatings on titanium alloys. *Biomaterials* 23, 2002: 4065-4077.
- [13] W. Xue, X. Liu, X. Zheng, C. Ding. Dissolution and mineralization of plasma sprayed wollastonite coatings with different crystallinity. *Surf Coat Technol* 200, 2005: 2420-2427.
- [14] Y. Acil H. Terheyden, A. Dunsche, B. Fleiner, S. Jepsen. Three-dimensional cultivation of human osteoblast-like cells on highly porous natural bone mineral. *J Biomed Mater Res* 51, 2000: 703-710.
- [15] S. Ni, J. Chang, L. Chou. A novel bioactive porous CaSiO_3 scaffold for bone tissue engineering. *J Biomed Mater Res* 76 A, 2006: 196-205.
- [16] J. Wei, F. Chen, J.W. Shin, H. Hong, C. Dai, J. Su. Preparation and characterization of bioactive mesoporous wollastonite-polycaprolactone composite scaffolds. *Biomaterials* 30, 2009: 1080-1088.
- [17] P.E. Ketting, M.J. Oursler, K.E. Wiegand, S.K. Bonde, T.C. Spelsberg, B.L. Riggs. A increases proliferation, differentiation, and transforming growth factor β production in normal adult human osteoblast-like cells *in vitro*. *J Bone Miner Res* 7, 1992: 1281-1289.
- [18] I.D. Xynos, A.J. Edgar, L.D.K. Buttery, L.L. Hench, J.M. Polak. Gene-expression profiling of human osteoblasts following treatment with the ionic products of Bioglass 45S5 dissolution. *J Biomed Mater Res* 55, 2001: 151-157.
- [19] J. Sun, L. Wei, X. Liu, J. Li, B. Li, G. Wang, F. Meng. Influences of ionic dissolution products of dicalcium silicate coating on osteoblastic proliferation, differentiation and gene expression. *Acta Biomater* 5, 2009: 1284-1293.
- [20] N.N. Ali, J. Rower, N.M. Reich. Constitutive expression of non-bone, liver/ kidney alkaline phosphatase in human osteocarcinoma cell lines. *J Bone Miner Res* 11, 1996: 512-520.
- [21] T. Matsuda, J.E. Davies. The *in vitro* response of osteoblasts to bioactive glass. *Biomaterials* 8, 1987: 275-284.

BADANIA BIOLOGICZNE WARSTW POWIERZCHNIOWYCH W ASPEKcie ZASTOSOWANIA NA PIERŚCIEŃ ZASTAWKI SERCA

M. GONSIOR^{1*}, R. KUSTOSZ¹, T. BOROWSKI², M. OSSOWSKI²,
M. SANAK³, B. JAKIEŁŁA³, E. CZARNOWSKA⁴, T. WIERZCHOŃ²

¹FUNDACJA ROZWOJU KARDIOCHIRURGII, ZABRZE

²WYDZIAŁ INŻYNIERII MATERIAŁOWEJ POLITECHNIKI WARSZAWSKIEJ

³COLLEGIUM MEDICUM UNIwersYTETU JagIELLOŃSKIEGO, KRAKÓW

⁴CENTRUM ZDROWIA DZIECKA W WARSZAWIE

* E-MAIL: GOSIAG@FRK.PL

Streszczenie

Oryginalna sztuczna komora wspomaganie serca POLVAD opracowana w Polsce, została zastosowana dotychczas w leczeniu ponad 210 pacjentów. Najdłuższe wspomaganie serca za pomocą komory POLVAD trwało ponad rok. Dla protezy tej opracowywana jest innowacyjna zastawka dyskowa, z nisko profilowym pierścieniem wykonanym ze stopu tytanu. Dla zminimalizowania trombogenności pierścienia zastawki opracowano dyfuzyjne warstwy powierzchniowe: azotowaną typu $TiN+Ti_2N+\alpha Ti(N)$ i tlenoazotowaną typu $TiO_2+TiN+Ti_2N+\alpha Ti(N)$, wytwarzane obróbką jarzeniową na potencjale plazmy. Trombogenność różnych kompozycji warstw została porównana w aspekcie aktywacji i adhezji płytek krwi do powierzchni biomateriału. Oceniono również wpływ metody sterylizacji biomateriału na intensywność adhezji trombocytów do jego powierzchni. Warstwy TiN oraz TiO_2 wykazały najniższą trombogenność, przy czym dla warstwy TiN korzystniejsza jest sterylizacja gazowa, podczas gdy dla warstwy TiO_2 - sterylizacja plazmowa.

[Inżynieria Biomateriałów, 102, (2011), 15-22]

Wprowadzenie

Mechaniczne protezy zastawek serca są wszczepiane jako implanty w miejsce uszkodzonej natywnej zastawki serca, ale stosowane są także w sztucznych sercach i komorach wspomaganie serca na całym świecie. W Polsce od 1999 r. stosowany jest system wspomaganie serca POLCAS, w skład którego wchodzi pozaustrojowa komora wspomaganie serca POLVAD i jednostka sterująca pracą komory. Do dnia dzisiejszego system POLCAS został zastosowany w leczeniu ponad 210 pacjentów w przypadkach ostrej niewydolności serca - jako pomost do regeneracji lub transplantacji serca. Najdłuższe wspomaganie serca za pomocą komór POLVAD trwało 403 dni. Komora POLVAD (RYS. 1a) początkowo wyposażona była w zastawki dyskowe firmy Sorin (RYS. 1b), dzisiaj wyposażona jest w zastawki dyskowe firmy Medtronic Hall (RYS. 1c). Cechą charakterystyczną tych zastawek jest wysoki profil elementu prowadzącego dysk zastawki - zlokalizowanego w centrum strumienia krwi przepływającej przez zastawkę. Element ten powoduje regionalne turbulencje przepływu krwi, zwiększając ryzyko powstawania skrzepin w obszarze pierścienia zastawki. W ramach programu „Polskie Sztuczne Serce” prowadzone są badania nad opracowaniem konstrukcji oryginalnej polskiej zastawki dyskowej dla protez serca, bazującej na projekcie zastawki prof. J. Molla [Moll J.J. patent USA 4.661.106, 1987; Moll J.J. patent USA 4.725.275, 1987].

BIOLOGICAL PROPERTIES OF SURFACE LAYERS FOR RING OF HEART VALVE APPLICATION

M. GONSIOR^{1*}, R. KUSTOSZ¹, T. BOROWSKI², M. OSSOWSKI²,
M. SANAK³, B. JAKIEŁŁA³, E. CZARNOWSKA⁴, T. WIERZCHOŃ²

¹FOUNDATION FOR CARDIAC SURGERY DEVELOPMENT, ZABRZE

²MATERIAL ENGINEERING DEPARTMENT,
WARSAW TECHNOLOGICAL UNIVERSITY

³COLLEGIUM MEDICUM JAGIELLONIAN UNIVERSITY, KRAKOW

⁴THE CHILDREN'S MEMORIAL HEALTH INSTITUTE IN WARSAW

* E-MAIL: GOSIAG@FRK.PL

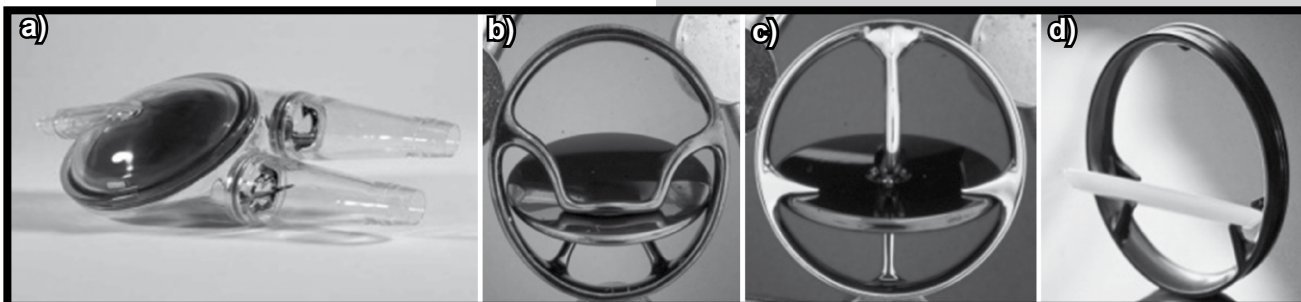
Abstract

The original ventricular assist device POLVAD developed in Poland was used in over 210 patients so far. The longest POLVAD heart assistance excided one year. The innovative tilting disk valve with low profile ring made of titanium is developed for POLVAD. To minimize the valve ring thrombogenicity the diffusive surface layers were manufactured: nitriding $TiN+Ti_2N+\alpha Ti(N)$ and oxynitriding $TiO_2+TiN+Ti_2N+\alpha Ti(N)$, in the glow discharge process on the plasma potential level. The thrombogenicity of different layers composition was compared regarding platelets activation and platelets adhesion to the material surface. The influence of material sterilization method on the platelets adhesion intensity was evaluated in addition. The nitriding TiN and oxynitriding TiO_2 layers have demonstrated the lowest thrombogenicity while the gas sterilization was the most profitable for nitriding layers - TiN and the plasma sterilization for oxynitriding layers - TiO_2 .

[Engineering of Biomaterials, 102, (2011), 15-22]

Introduction

The mechanical heart prostheses are used as the implants in the place of damaged native heart valve, but they are also used in the ventricular assist devices and artificial hearts all over the world. The original mechanical circulatory system POLCAS is clinically used since 1999. It consists of the ventricular assist device POLVAD and the driving unit POLPDU. Until now it was used in more than 210 cases of the end stage heart failure support - as the bridge to the heart regeneration or heart transplantation. The longest effective heart assistant with ventricular assist device POLVAD lasted 403 days. The ventricular assist device POLVAD (FIG. 1a) firstly was provided with Sorin tilting disc valves (FIG. 1b), currently the tilting disk Medtronic Hall valves (FIG. 1c) are used. The feature of these valves is high profile of the elements holding the valve disc - located in the centre of the blood flow. The holding disc element causes local blood flow turbulences increasing the risk of thrombus formation in the valve ring area. Within the national research program "Polish Artificial Heart" the new construction tilting disk valve is performed pursuant originally proof. J. Moll construction [Moll J.J. patent USA 4.661.106, 1987; Moll J.J. patent USA 4.725.275, 1987]. The ring elements holding the valve disc are small and they are located very close to the valve ring releasing the blood flow area from disturbing blood flow profiles (FIG. 1d).



RYS. 1. a) sztuczna komora POLVAD; b) zastawka dyskowa Sorin; c) zastawka dyskowa Medtronic Hall; d) nowa zastawka dyskowa.

FIG. 1. a) ventricular assist device POLVAD; b) tilting disc Sorin valve; c) tilting disc Medtronic Hall valve; d) new tilting disc valve.

Pierścień tej zastawki prowadzi dysk za pomocą małych elementów (RYS. 1d), zlokalizowanych przy ścianie pierścienia, uwalniając przestrzeń przepływu krwi przez zastawkę od profili wywołujących zaburzenia przepływu.

Ze względu na wysoką biogodność oraz wysoką odporność na biodegradację tytanu i jego stopów [1-3] w opracowywanej zastawce przewidywane jest wykorzystanie tych materiałów na pierścieniu zastawki. Opisująca w literaturze wysoka trombogenicność tytanu i jego stopów [4,5] stanowi podstawę badań nad opracowaniem warstw modyfikujących powierzchnię pierścienia zastawki w aspekcie zapewnienia niskiej trombogenicności powierzchni biomateriału przy jednoczesnym zachowaniu dobrych właściwości mechanicznych tytanu i jego stopu. W pracy przeprowadzono badania porównawcze trombogenicności trzech warstw azotowanych, tlenoazotowanych i tlenowęglaozotowanych z przypowierzchniową strefą faz: TiN, TiO₂, Ti(OCN) wytworzonych na podłożu stopu tytanu Ti6Al4V metodą niskotemperaturowych obróbek jarzeniowych. Trombogenicność oceniano poprzez porównanie stopnia, w jakim powierzchnia biomateriału aktywuje trombocyty. Oceny aktywacji trombocytów dokonano w warunkach statycznej i dynamicznej ekspozycji powierzchni biomateriału do krwi. W pracy wykonano również analizę wpływu metody sterylizacji na własności trombogeniczne powierzchni wytworzonych warstw.

Material i metody

Dyfuzyjne warstwy powierzchniowe zostały wytworzone na Wydziale Inżynierii Materiałowej Politechniki Warszawskiej w procesach azotowania, tlenoazotowania i tlenowęglaozotowania. Trzy warstwy dyfuzyjne o strukturze nanokrystalicznej i grubości rzędu kilku μm typu (skład fazowy warstw od powierzchni): TiN+Ti₂N+ α Ti(N), TiO₂+TiN+Ti₂N+ α Ti(N) oraz Ti(OCN)+TiN+Ti₂N+ α Ti(N) zostały wytworzone w niskotemperaturowych procesach obróbek jarzeniowych w temperaturze poniżej 700°C na wypolerowanych dyskach ze stopu Ti6Al4V (o średnicy 14,5 mm i grubości 3 mm).

Badanie topografii i struktury powierzchni

Mikrostrukturę warstwy oceniono w badaniach na mikroskopie skaningowym (HITACHI S-3500). Pomiary chropowatości powierzchni wykonano profilometrem (Wyko NT9300) oraz na mikroskopie sił atomowych (Veeco model Multimode Nanoscope V).

Badania trombogenicności powierzchni

Badania trombogenicności powierzchni wykonano w dwóch różnych modelach warunków kontaktu krwi z powierzchnią biomateriału: statycznych i dynamicznych.

Due to high biocompatibility and high biodegradation resistance of titanium and its alloys [1-3], using these materials to the valve ring construction is taken into account. High thrombogenicity of titanium and its alloys [4,5] reported in the literature, is a basis for development of modified layers on the valve ring surface, in order to provide low biomaterial surface thrombogenicity and protect the good titanium mechanical properties at the same time. The comparative thrombogenicity tests of the nitriding, oxynitriding and carbooxynitriding layers with the surface phase areas: TiN, TiO₂ and Ti(OCN) produced on the titanium alloy in the low temperature glow discharge process were done. The thrombogenicity was evaluated by the comparison of the platelets activation due to the biomaterial surface contact. The platelets activation in the conditions of static and dynamic biomaterials surface exposure to the blood was evaluated. The influence of sterilization method influence on the layers surface thrombogenicity was also evaluated.

Materials and methods

The diffusive layers were produced by the Material Engineering Department of Warsaw Technological University in the nitriding, oxynitriding and carbooxynitriding processes. The three diffusive nano-crystalline layers with micrometric thickness type (the layers phase composition from the surface): TiN+Ti₂N+ α Ti(N), TiO₂+TiN+Ti₂N+ α Ti(N) and Ti(OCN)+TiN+Ti₂N+ α Ti(N) were produced in the low temperature glow discharge process in the temperature below 700°C, on the polished disk surface made of titanium alloy Ti6Al4V (14.5 mm diameter; 3 mm thickness).

Surface topography and structure tests

The layer microstructure was evaluated by the scanning microscope examination (HITACHI S-3500). The surface roughness was evaluated using the profilometry (WykoNT9300) and the atomic force microscope (Veeco Multimode Nanoscope V).

The surface thrombogenicity tests

The surface thrombogenicity tests were done in the different conditions: static and dynamic biomaterials surface exposure to the blood.

In the static thrombogenicity tests the biomaterial samples were incubated for 20 minutes and 2 hours in the temperature of 37°C in 400 μl of rich platelets plasma, which was prepared from the blood of two healthy donors. The cells adhered to the samples surface were fixed with 2.5% glutaraldehyde and dehydrated with increasing concentration of ethylene alcohols and propylene oxide. Then the cells were covered with the gold layer of 10-15 nm thickness (Fine coater Jeol JFC 1200).

Badania w warunkach statycznych polegały na ekspozycji próbek biomateriału przez czas 20 minut i 2 godzin w temperaturze 37°C w 400 µl osocza bogato płytkowego, przygotowanego z krwi dwóch zdrowych dawców. Komórki zaadherowane na powierzchni próbek utrwalane w 2,5% glutaraldehydzie w buforze kaskodowym odwadniano w alkoholach etylowych o rosnących stężeniach i w tlenku propylenu. Następnie napyłano warstwą złota grubości ok. 10-15 nm (Fine coater Jeol JFC 1200). Preparaty badano w mikroskopie skaningowym. Fotografowano losowo wybrane mikroobszary strefy brzegowej i części centralnej próbek. W dalszej kolejności wykonano analizę morfometryczną obserwowanych komórek. Za pomocą badania skaningowej mikroskopii elektronowej analizowano morfologię oraz rozmieszczenie płytek i agregatów płytkowych. Następnie za pomocą programu morfometrycznego CellP (Olympus) zliczano w badanych mikroobszarach zaadherowane płytki i agregaty płytowe ($n/1420 \mu\text{m}^2$).

Badania w warunkach dynamicznych polegały na wytworzeniu modelu naprężeń ścinających na granicy powierzchni biomateriału z krwią odpowiadających tym, jakie oddziałują na krew przepływającą przy ścianach naczyń tętniczych średniej wielkości. Model takich zjawisk jest wykorzystywany do pomiaru adhezji trombocytów w urządzeniu diagnostycznym Impact-R (DiaMed, Szwajcaria). Nad próbką materiału (dysk o średnicy 14,5 mm bez i z powierzchniową warstwą) 130 µl krwi wprowadzane jest w wirowanie z prędkością 720 obr/min przez czas 300 sekund. Po ekspozycji krew poddawana była ocenie pod kątem: liczebności krążących trombocytów, liczebności agregatów płytkowych (z różnicowaniem na duże i małe) oraz poziomu aktywacji trombocytów wyrażanej ekspresją Selktyny-P oraz receptora GpIIb/IIIa - w badaniu cytometrii przepływowej.

Rezultaty

Mikrostruktura i topografia powierzchni

Warstwy wytworzone w procesach azotowania, tlenoazotowania i tlenowęglaozotowania jarzeniowego wykazywały jednorodną strukturę w całym przekroju próbki (RYS. 2), posiadały jednorodną topografię powierzchni (RYS. 3,4, TABELA 1) i mikrotwardość powierzchni (kolejno): TiN – 1200 HV 0.05, TiO₂ – 880 HV 0.02, Ti(OCN) – 1300 HV 0.05.

Trombogenność powierzchni w warunkach statycznych

Adhezja płytek do powierzchni biomateriału

Pierwszym badanym aspektem była adhezja płytek krwi do powierzchni próbek biomateriałów po statycznej ekspozycji do osocza bogato płytkowego. Zaobserwowano różnice w adhezji płytek w strefie brzegowej w porównaniu ze strefą centralną wszystkich badanych próbek. Mniejsza ilość płytek krwi zaadherowała na krawędziach niż w środku próbek (RYS. 5). Liczba płytek krwi zaadherowanych na próbkach istotnie zależała od sposobu ich sterylizacji w przypadku warstw tlenowęglaozotowanych – Ti(OCN) oraz stopu tytanu (Ti), przy czym była większa na płytkach sterylizowanych gazowo niż plazmowo (RYS. 6,7). Analiza porównawcza badanych biomateriałów wykazała najmniejszą adhezję płytek krwi na próbkach z warstwami azotowanymi – TiN i tlenoazotowanymi – TiO₂.

The preparations were tested in scanning microscope. The micro areas of the sample edge and sample centre randomly chosen were photographed. Afterwards the morphometric analysis of the observed cells was done. The platelets morphology, platelets and platelets aggregates arrangement were analyzed by the scanning electron microscope. Using the morphometric program CellP (Olympus) the adhered platelets and platelets aggregates in tested micro areas were counted ($n/1420 \mu\text{m}^2$).

The dynamic thrombogenicity tests consists in the shear-stress model creating in the blood layer contacting biomaterial surface, similar like the shear-stresses affecting on the blood flowing near the vessel wall in the medium size arteries. The shear-stress model is used to test the platelets adhesion in the diagnostic equipment Impact-R (DiaMed, Switzerland). Over the material sample (the disc with and without diffusive layer - diameter 14.5 mm) 130 µl of blood is rotating with velocity 720 rpm/min for 300 s. After the exposure the blood parameters were analyzed: the number of platelets consequently circulating in the blood, number of the platelets aggregates (small and big platelets aggregates) and the platelets activation examined by the expression of GpIIb/IIIa and selectin-P receptors in the flow cytometry test.

Results

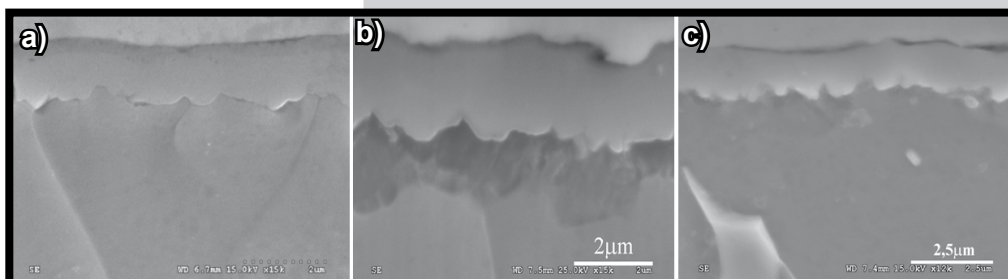
Surface microstructure and topography

The layers produced in the glow discharge nitriding, oxy-nitriding and carboxynitriding process, have the homogeneous structure in the whole sample cross-section (FIG. 2), homogeneous surface topography (FIG. 3,4, TABLE 1) and micro hardness of the surface (in sequence): TiN – 1200 HV 0.05, TiO₂ – 880 HV 0.02, Ti(OCN) – 1300 HV 0.05.

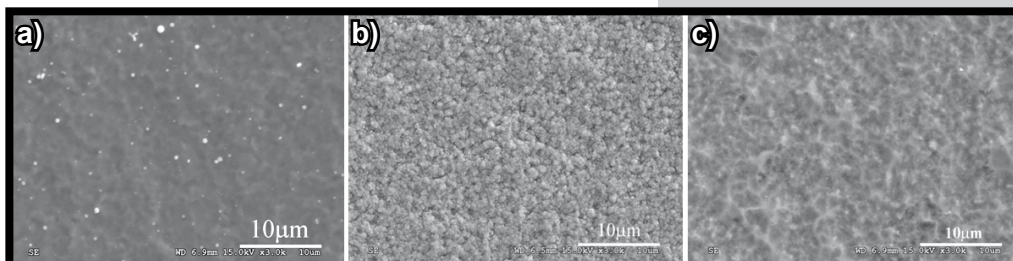
Static surface thrombogenicity tests

Platelets adhesion to the biomaterial surface

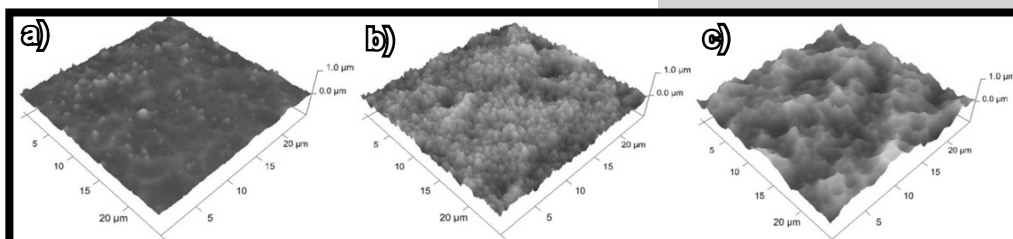
The first analyzed parameter was platelets adhesion to the biomaterials surface, after static exposure to the platelet rich plasma. The platelets adhesion differences in the sample peripheral area comparing with the sample central area were observed. The lower number of adhered platelets was observed in the samples periphery than in the samples centre (FIG. 5). The number of adhered platelets essentially depended on sterilization method in the case of carboxynitriding layer - Ti(OCN) and titanium alloy (Ti6Al4V) - the higher number of adhered platelets was observed after gas sterilization than after plasma sterilization (FIG. 6,7). The comparative analysis of tested biomaterials showed the lowest platelets adhesion on the nitriding - TiN and oxynitriding - TiO₂ layers.



RYS. 2. Mikrostruktura stereometryczna warstwy na stopie tytanu Ti6Al4V: a) TiN+Ti₂N+αTi(N); b) TiO₂+TiN+Ti₂N+αTi(N); c) Ti(OCN)+TiN+Ti₂N+αTi(N).
FIG. 2. Microstructure of the layers on the titanium alloy Ti6Al4V: a) TiN+Ti₂N+αTi(N); b) TiO₂+TiN+Ti₂N+αTi(N); c) Ti(OCN)+TiN+Ti₂N+αTi(N).



RYS. 3. Topografia warstwy na stopie tytanu Ti6Al4V: a) TiN+Ti₂N+αTi(N); b) TiO₂+TiN+Ti₂N+αTi(N); c) Ti(OCN)+TiN+Ti₂N+αTi(N).
FIG. 3. Topography of the layers on the titanium alloy Ti6Al4V: a) TiN+Ti₂N+αTi(N); b) TiO₂+TiN+Ti₂N+αTi(N); c) Ti(OCN)+TiN+Ti₂N+αTi(N).



RYS. 4. Topografia warstwy na stopie tytanu Ti6Al4V w badaniu mikroskopii sił atomowych: a) TiN+Ti₂N+αTi(N); b) TiO₂+TiN+Ti₂N+αTi(N); c) Ti(OCN)+TiN+Ti₂N+αTi(N).
FIG. 4. Topography of the layers on the titanium alloy Ti6Al4V by the atomic forces microscopy: a) TiN+Ti₂N+αTi(N); b) TiO₂+TiN+Ti₂N+αTi(N); c) Ti(OCN)+TiN+Ti₂N+αTi(N).

TABELA 1. Parametry chropowatości powierzchni stopu tytanu bez i z wytworzonymi warstwami.
TABLE 1. The stereometric parameters of the titanium alloy surface with the diffusive layers.

| Parametr chropowatości powierzchni / Surface roughness parameters [μm] | Ti6Al4V | TiN | TiO ₂ | Ti(OCN) |
|--|---------|-------|------------------|---------|
| Ra | 0,035 | 0,138 | 0,673 | 0,197 |
| Rq | 0,045 | 0,180 | 0,886 | 0,252 |
| Rz | 0,363 | 1,93 | 8,19 | 2,41 |

Agregacja płytek na powierzchni biomateriału

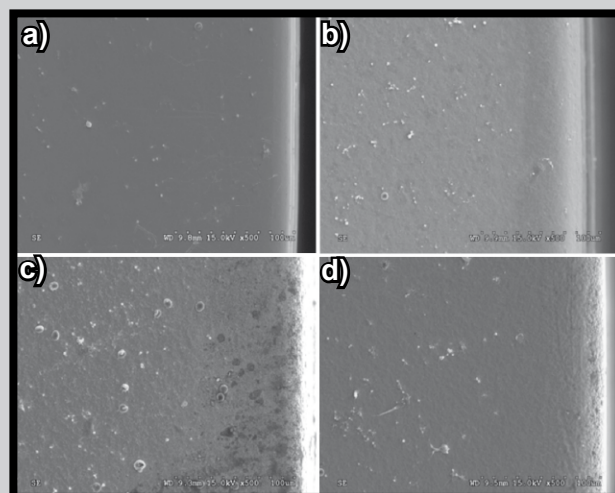
Drugim badanym aspektem była liczebność agregatów płytkowych występujących na powierzchni biomateriału po ekspozycji statycznej do osocza bogato płytkowego. W badaniu mikroskopii elektronowej w części centralnej płytek występowała większa liczba agregatów niż w strefie brzegowej - niezależnie od sposobu sterylizacji. W czasie 20 min inkubacji płytek krwi nie obserwowano znamienego wpływu sterylizacji na powstawanie agregatów płytkowych. Natomiast dwugodzinna inkubacja wskazuje, że mniej agregatów tworzy się na powierzchni warstw tlenoazotowanych - TiO₂ i stopie tytanu - Ti6Al4V sterylizowanych gazowo niż plazmowo, natomiast na powierzchni warstw azotowanych - TiN i tlenowęglazotowanych - Ti(OCN) odwrotnie (RYS. 8,9).

Morfologia płytek

Ocenie podlegała również morfologia zaadherowanych do powierzchni biomateriału płytek krwi. Rozpłaszczenie płytek krwi i/lub formowanie rozplaszczonych filopodiów są wyrazem ich aktywacji. Obrazy uzyskane w mikroskopii elektronowej wskazują, że na próbkach sterylizowanych gazowo zaadherowane płytki krwi są mniej rozplaszczone i charakteryzuje je obecność długich wypustek (RYS. 10,11).

Platelets aggregation on the biomaterial surface

The number of platelets aggregates on the biomaterial surface was tested after static exposure to the platelet rich plasma. The electron microscopy showed that there is higher number of platelets aggregates in the samples centre than in the periphery samples irrespective of sterilization method. There was not observed any important influence of sterilization method on platelets aggregation after 20 min of incubation. Whereas 2 hours incubation resulted in smaller number of platelets aggregated on the oxynitriding layers - TiO₂ and titanium alloy -Ti6Al4V gas sterilized, while on the nitriding layers - TiN and carboxynitriding layers - Ti(OCN) opposite relation was observed (FIG. 8,9).

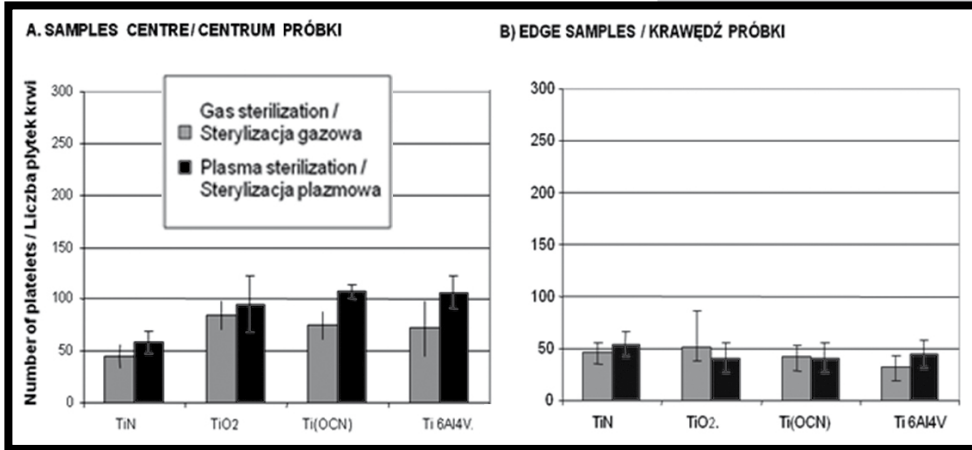


RYS. 5. Strefa brzegowa próbki ze stopu tytanu Ti6Al4V (a) oraz z warstwami: azotowaną (TiN) (b), tlenoazotowaną (TiO₂) (c) i tlenowęglazotowaną (Ti(OCN)) (d).

FIG. 5. The peripheral part of the samples made of titanium alloy Ti6Al4V (a) and nitriding layer (TiN) (b), oxynitriding layer (TiO₂) (c) and carboxynitriding layer (Ti(OCN)) (d).

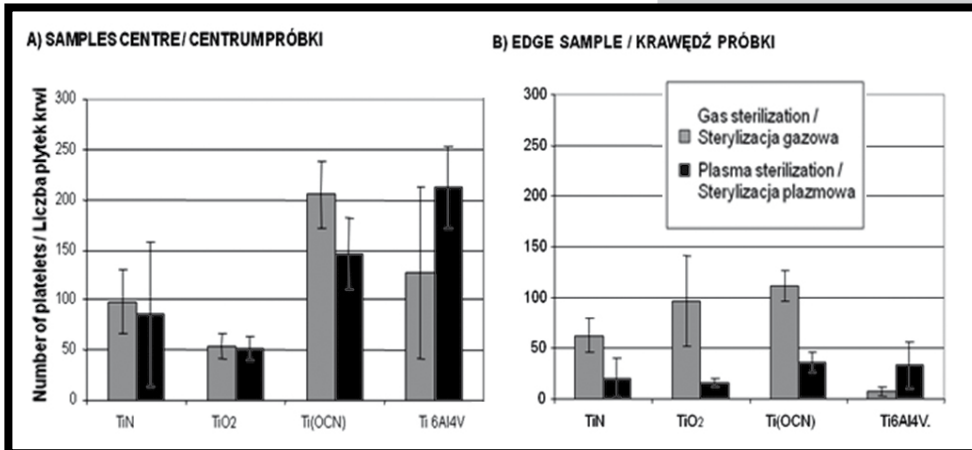
Platelets morphology

Morphology of platelets adhered to the biomaterials surface was also tested. Platelets flattening and/or platelets pseudopodia expansion are the platelets activation evidences. The electron microscopy showed that adhered platelets are less flatten on the gas sterilized surfaces and they have a lot of long pseudopodia (FIG. 10,11).



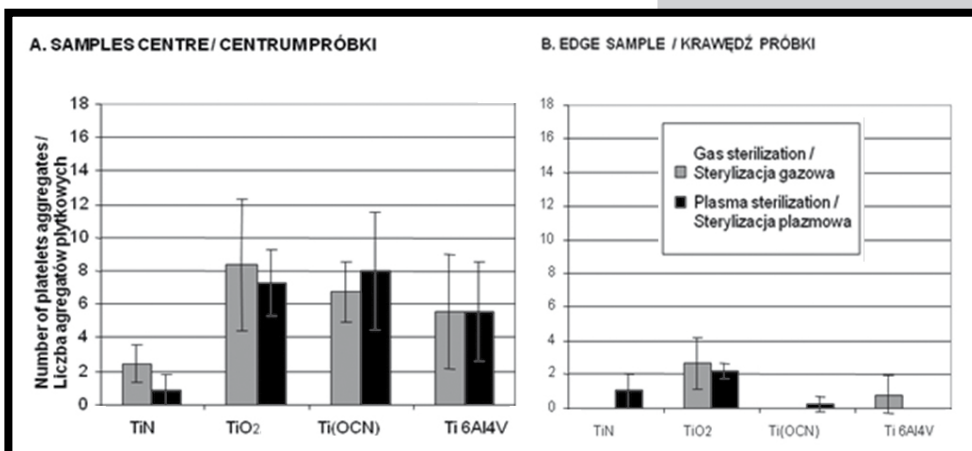
RYS. 6. Liczba płytek krwi w mikroobszarach 1,42 mm² badanych biomateriałów po 20 min. inkubacji z osoczem bogato płytkowym.

FIG. 6. The platelets number in the micro areas 1.42 mm² of tested biomaterials after 20 min incubation in platelet rich plasma.



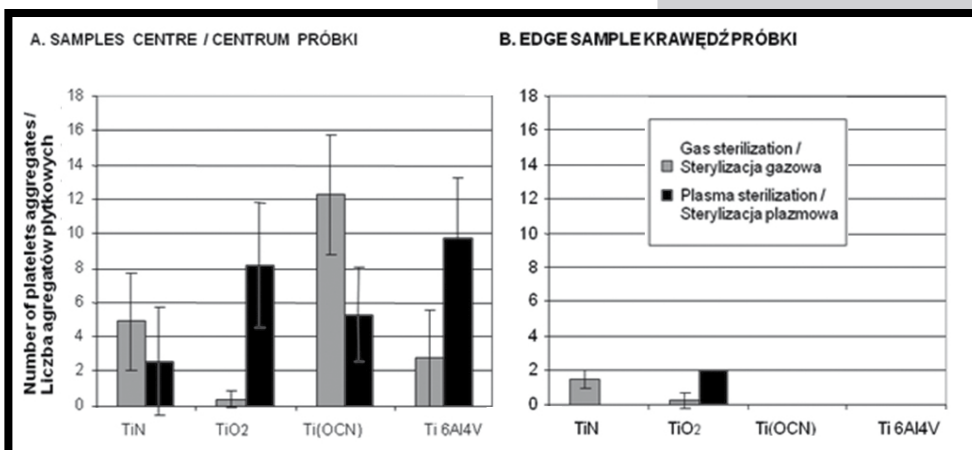
RYS. 7. Liczba płytek krwi w mikroobszarach 1,42 mm² badanych biomateriałów po 2 godz. inkubacji z osoczem bogato płytkowym.

FIG. 7. The platelets number in the micro areas 1.42 mm² of tested biomaterials after 2 hours incubation in platelet rich plasma.



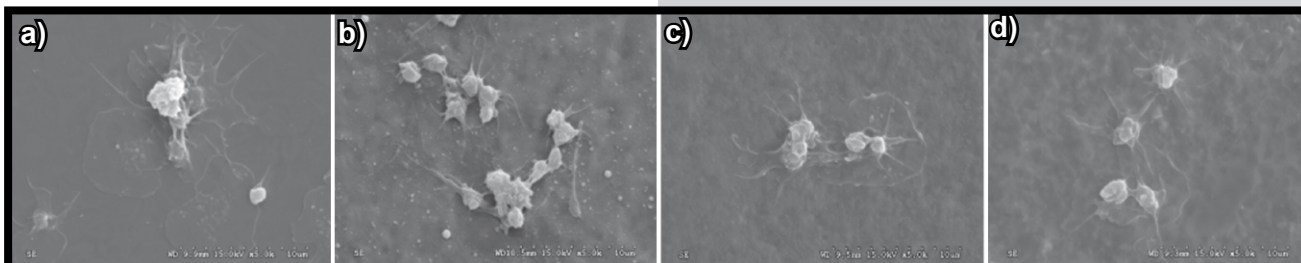
RYS. 8. Liczba agregatów płytkowych w mikroobszarach o powierzchni 1,42 mm² badanych biomateriałów po 20 min inkubacji z osoczem bogato płytkowym.

FIG. 8. The platelets aggregates number in the micro areas 1.42 mm² tested biomaterials after 20 min incubation in platelet rich plasma.

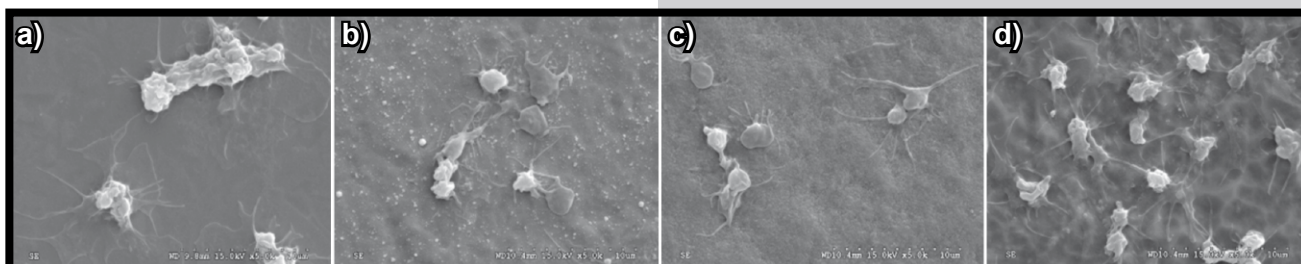


RYS. 9. Liczba agregatów płytkowych w mikroobszarach o powierzchni 1,42 mm² badanych biomateriałów po 2 godz. inkubacji z osoczem bogato płytkowym.

FIG. 9. The platelets aggregates number in the micro areas 1.42 mm² tested biomaterials after 2 hours incubation in platelet rich plasma.



RYS. 10. Morfologia płytek krwi zaadherowanych na badanych biomateriałach sterylizowanych plazmowo w nadtlenu wodoru: a) stop tytanu Ti6Al4V, b) azotek tytanu, c) tlenoazotek tytanu, d) tlenowęgloazotek tytanu.
FIG. 10. Morphology of platelets adhered on the plasma sterilized biomaterials surfaces: a) titanium alloy Ti6Al4V, b) nitriding layer, c) oxynitriding layer, d) carboxynitriding layer.



RYS. 11. Morfologia płytek krwi zaadherowanych na badanych biomateriałach sterylizowanych w tlenku etylenu: a) stop tytanu Ti6Al4V, b) azotek tytanu, c) tlenoazotek tytanu, d) tlenowęgloazotek tytanu.
FIG. 11. Morphology of platelets adhered on the gas sterilized biomaterials surfaces: a) titanium alloy Ti6Al4V, b) nitriding layer, c) oxynitriding layer, d) carboxynitriding layer.

Trombogenność powierzchni w warunkach dynamicznych

Badania przeprowadzono dla wszystkich warstw (TiN, TiO₂ i Ti(OCN)) oraz dla stopu tytanu Ti6Al4V, a także dla materiałów referencyjnych: polistyrenu, którego powierzchnię firma DiaMed rekomenduje w metodzie badań urządzenia jako odpowiadającą najlepiej warunkom panującym w pobliżu ścian naczyń tętniczych oraz dla poliuretanu z jakiego aktualnie wytwarzane są pozaustrojowe komory wspomaganie serca.

W badaniach trombogenności w warunkach dynamicznych zaobserwowano, że największa liczba płytek krwi po ekspozycji krąży w kontakcie z powłokami TiN oraz TiO₂. Odpowiednio również dla tych dwóch warstw liczba agregatów płytkowych krążących w krwi była najniższa. Warto jednak zauważyć, że chociaż dla warstwy tlenowęgloazotowanej (zewnętrzna strefa warstwy Ti(OCN)) odnotowano wyższą agregację trombocytów, to wszystkie warstwy wytworzone na powierzchni stopu tytanu mają większą liczebność krążących trombocytów i mniejszy udział agregatów płytkowych w porównaniu do wypolerowanego (o najniższej chropowatości – TABELA 1) stopu Ti6Al4V (RYS. 12,13).

Analizie poddano również stopień, w jaki badane powierzchnie aktywowały płytki krwi przepływającej nad powierzchnią. Oznaczano aktywność płytek wyrażaną ekspresją: selektyny-P (RYS. 14) oraz receptora integryny IIb/IIIb (RYS. 15). Najbardziej płytki aktywowała powierzchnia warstwy tlenowęgloazotowanej – Ti(OCN), podczas gdy najslabiej warstwa tlenoazotowana – TiO₂ oraz wypolerowana powierzchnia stopu tytanu.

Dla badań trombogenności w warunkach dynamicznych dokonano również porównawczej analizy: liczebności płytek krwi i agregatów płytkowych krążących we krwi, płytek krwi i stopnia ich aktywacji (RYS. 16,17,18). Dla lepszego zrozumienia własności trombogennych badanych powierzchni biomateriałów przeanalizowano jednoczesność występowania różnych zjawisk odpowiedzialnych za trombogenność. Między innymi porównano ilość płytek krwi i agregatów płytkowych krążących we krwi po kontakcie z powierzchnią biomateriału z wywołaną jednocześnie aktywacją krwi spowodowaną kontaktem z biomateriałem.

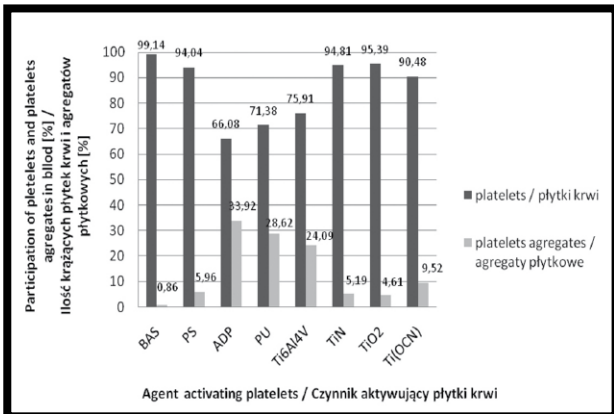
The dynamic thrombogenicity tests

The dynamic thrombogenicity tests were done for all tested layers (TiN, TiO₂, Ti(OCN)), titanium alloy Ti6Al4V and reference materials such as polystyrene and polyurethane. Polystyrene is recommended by DiaMed Company as the material which simulates in the best way the physiological conditions in the human arteries. Polyurethane is currently used as the construction material of ventricular assist devices.

The dynamic thrombogenicity tests showed that the highest platelets number consequently circulate in the blood in contact with nitriding and oxynitriding layers. The number of platelets aggregates observed in the blood after contact with TiN and TiO₂ was the lowest. Although the higher platelets aggregation was observed in the blood after contact with carboxynitriding layers (the external layer area Ti(CON)), the all three diffusive layers developed on the titanium alloy surface have more circulating platelets and lowest contribution in platelets aggregates than polished titanium alloy (with the lowest roughness – TABLE 1, FIG. 12,13).

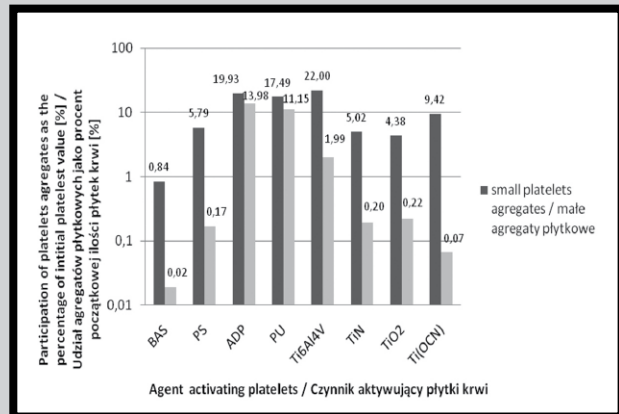
The platelets activation caused by tested surfaces was investigated by testing the selectin-P (FIG. 14) and receptor GPIIb/IIIa (FIG. 15) expression. Higher platelets activation was observed in the blood after contact with carboxynitriding layer Ti(OCN), whereas the lowest platelets activation was observed in the blood after contact with oxynitriding layer TiO₂ and polished titanium alloy surface.

In the dynamic thrombogenicity tests the comparative analysis was done: the number of platelets compared with the number of platelets aggregates circulating in the blood and with the platelets activation (FIG. 16,17,18). For better understanding the thrombogenic properties of tested biomaterials surfaces, the simultaneity of different phenomena responsible for thrombogenicity occurrence was analyzed. Among other things platelets and aggregates number circulating in the blood after contact with biomaterials surface was compared to blood activation due to contact with biomaterial.



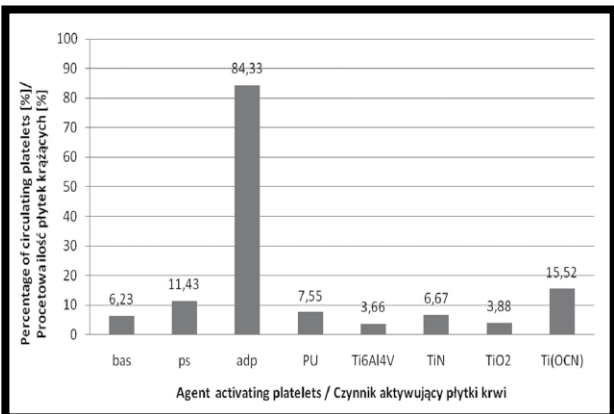
RYS. 12. Porównanie liczby płytek krwi z liczbą agregatów płytkowych w krwi po ekspozycji dla naprężeń ścinających.

FIG. 12. Platelets and platelets aggregates number circulating in the blood after contact with biomaterials surfaces.



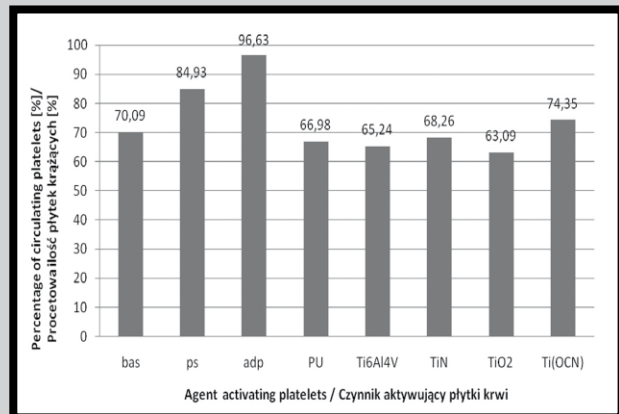
RYS. 13. Porównanie liczby małych i dużych agregatów płytkowych w krwi po ekspozycji dla naprężeń ścinających.

FIG. 13. Number of small and big platelets aggregates circulating in the blood after contact with biomaterials surfaces.



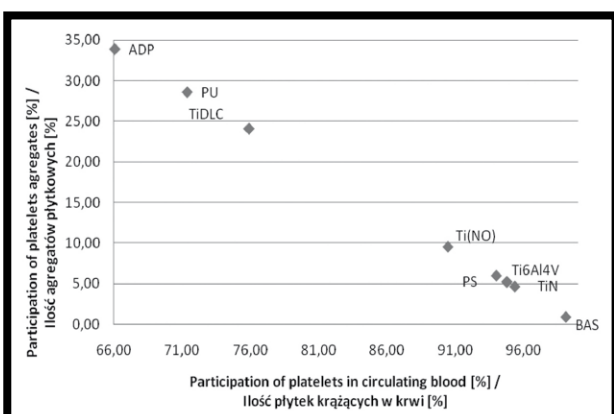
RYS. 14. Udział procentowy zaktywowanych płytek w krwi krążącej po ekspozycji do naprężeń ścinających, określony na podstawie ekspresji selektyny-P.

FIG. 14. Percentage number of activated platelets in the circulating blood – selectin-P expression.



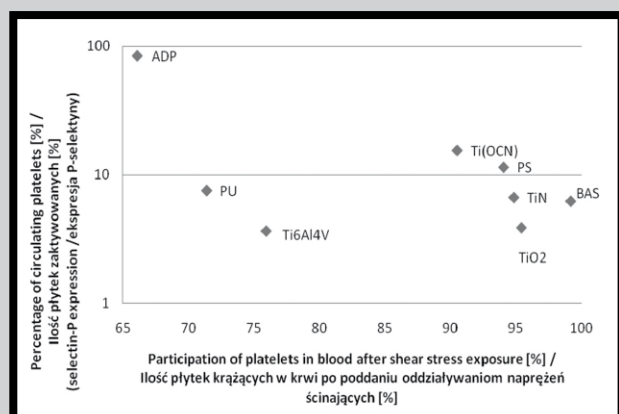
RYS. 15. Udział procentowy zaktywowanych płytek w krwi krążącej po ekspozycji do naprężeń ścinających, określony na podstawie ekspresji receptora GPIIb/IIIa.

FIG. 15. Percentage number of activated platelets in the circulating blood – GPIIb/IIIa expression.



RYS. 16. Poziom agregatów płytkowych i płytek krwi krążących we krwi po ekspozycji na naprężenia ścinające.

FIG. 16. Platelets and platelets aggregates circulating in the blood after contact with the biomaterial surface.

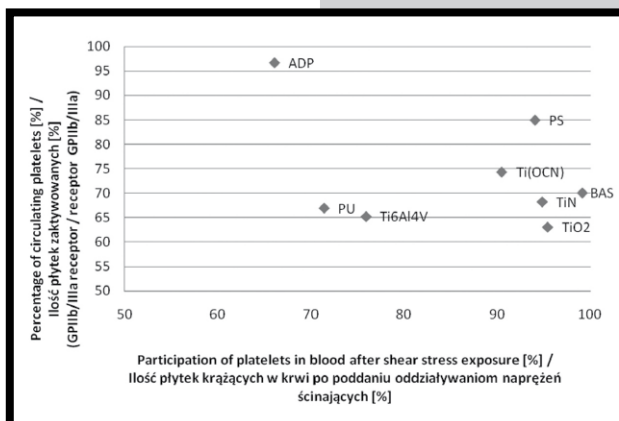


RYS. 17. Aktywacji płytek (ekspresja selektyny-P) w relacji do liczby płytek krążących we krwi po kontakcie z powierzchnią biomateriału.

FIG. 17. Platelets activation (selectin-P expression) related to platelets number circulating in the blood after contact with the biomaterial surface.

Podsumowanie

Badania porównawcze wskazują, że dla uzyskania lepszych właściwości atrombogenicznych powierzchni wytworzonych biomateriałów korzystniejszą sterylizacją dla warstw tlenoazotowanych – $\text{TiO}_2 + \text{TiN} + \text{Ti}_2\text{N} + \alpha\text{Ti(N)}$ i stopu tytanu Ti6Al4V jest sterylizacja gazowa, a dla warstw azotowanych $\text{TiN} + \text{Ti}_2\text{N} + \alpha\text{Ti(N)}$ i tlenowęglonitrowanych $\text{Ti(OCN)} + \text{TiN} + \text{Ti}_2\text{N} + \alpha\text{Ti(N)}$ sterylizacja plazmowa. Takie metody przyczyniają się do mniejszej adhezji i agregacji płytek. Badania na krwi wykazały dobre własności atrombogeniczne wytworzonych warstw dyfuzyjnych azotowanych – TiN i tlenoazotowanych – TiO_2 na stopie tytanu Ti6Al4V.



RYS. 18. Aktywacji płytek (ekspresja receptora GPIIb/IIIa) w relacji do liczby płytek krążących we krwi po kontakcie z powierzchnią biomateriału.

FIG. 18. Platelets activation (receptor GPIIb/IIIa expression) related to platelets number circulating in the blood after contact with the biomaterial surface.

Summary

The comparative investigation presented that to obtain better athrombogenic properties of biomaterials surfaces the gas sterilization is more suitable for oxynitriding layer ($\text{TiO}_2 + \text{TiN} + \text{Ti}_2\text{N} + \alpha\text{Ti(N)}$) and titanium alloy – Ti6Al4V, and plasma sterilization – for nitriding ($\text{TiN} + \text{Ti}_2\text{N} + \alpha\text{Ti(N)}$) and carboxynitriding layers ($\text{Ti(OCN)} + \text{TiN} + \text{Ti}_2\text{N} + \alpha\text{Ti(N)}$). These sterilization methods contribute to lower platelets adhesion and aggregation.

The blood tests confirmed good athrombogenic properties of developed layers: nitriding – TiN and oxynitriding – TiO_2 on the titanium alloy Ti6Al4V.

Podziękowania

Praca została wykonana w ramach projektu rządowego „Polskie Sztuczne Serce” nr 01/WK/P01/001/SPB-PSS/2008.

Acknowledgement

The researches were done as a part of government project “Polish Artificial Heart” number 01/WK/P01/001/SPB-PSS/2008.

Piśmiennictwo

- [1] C.Elias, J.Lima, R.Valiev, M.Meyers: Biomedical Applications of Titanium and its Alloys, JOM Journal of the Minerals, Metals and Materials Society, 2008, Volume 60, Number 3, 46-49, DOI: 10.1007/s11837-008-0031-1.
- [2] J.Marciniak, Z.Paszenda: Biotolerancja biomateriałów metalicznych, Spondyloimplantologia zaawansowanego leczenia kręgosłupa System DERO. Red. L.F. Ciupik, D. Zarzycki. Polska Grupa DERO, Stowarzyszenie studiów i badań kręgosłupa, 133-142, 2004.
- [3] M. Textor, C. Sittig, V. Frauchiger, S. Tosatti, D.M. Brunette, Properties and Biological Significance of Natural Oxide Films on Titanium and Its Alloys, „Titanium in Medicine: Material Science, Surface Science, Engineering, Biological Responses and Medical Applications”, Springer Verlag, Heidelberg and Berlin; pp 171-230, 2001.

References

- [4] Laczkovics A, Heidt M, Oelert H, Laufer G, Greve H, Pomar JL, et al.: Early clinical experience with the On-X prosthetic heart valve, J Heart Valve Dis 2001;10(1):94-9.
- [5] F.Schoen, J.Titus, G.Lawrie: Bioengineering aspects of heart valve replacement, Annals of Biomedical Engineering USA, 1982, vol. 10, pp. 97-128.
- [6] T. Borowski, A. Sowińska, M. Ossowski, E. Czarnowska, T. Wierchoń: The process of glow discharge assisted oxynitriding of titanium alloy in aspect of its application in artificial heart components, Inżynieria Materiałowa 3 (2010) 751-754.

ANALIZA UWARUNKOWAŃ DECYDUJĄCYCH O ODPORNOŚCI SZKLIWA NA ZUŻYCIĘ CZĘŚĆ II: BADANIA WARSTWY WIERZCHNIEJ ORAZ MIKROTWARDZOŚCI SZKLIWA ZĘBOWEGO

WOJCIECH RYNIEWICZ¹, MARIOLA HERMAN², ANNA M. RYNIEWICZ^{1,3*}

¹ UNIwersYTET JAGIELLOŃSKI COLLEGIUM MEDICUM,
WYDZIAŁ LEKARSKI, KATEDRA PROTETYKI STOMATOLOGICZNEJ,
UL. MONTELUPICH 4, 31-155 KRAKÓW

² V WOJSKOWY SZPITAL KLINICZNY Z POLIKLINIKĄ,
ODDZIAŁ STOMATOLOGII ZACHOWAWCZEJ Z ENDODONCJĄ,
UL. WROCŁAWSKA 1-3, 30-901 KRAKÓW

³ AKADEMIA GÓRNICZO HUTNICZA,
WYDZIAŁ INŻYNIERII MECHANICZNEJ I ROBOTYKI,
AL. MICKIEWICZA 30, 30-059 KRAKÓW

* E-MAIL: GHRYNIEW@CYF-KR.EDU.PL

Streszczenie

Opracowanie stanowi kontynuację zagadnień, w których wskazano uwarunkowania decydujące o odporności szkliwa naturalnego na zużycie. W części II opisano badania obejmujące ocenę stereometrii warstwy wierzchniej szkliwa z wykorzystaniem mikroskopii sił atomowych (AFM) oraz wyznaczenie mikrotwardości zębów z wykorzystaniem metody Oliver & Pharr.

Analizę statystyczną parametrów morfologicznych szkliwa z zębów przedtrzonowych i trzonowych przeprowadzono z zastosowaniem programu Scanning Probe Image Processor. Analiza pozwoliła zidentyfikować obrazy o różnym zakresie skanowania, wyznaczyć parametry chropowatości powierzchni na poziomie nano oraz różnicować struktury w sposób jakościowy i ilościowy. Zmiany chropowatości miały charakter okresowy o zbliżonych parametrach amplitudy, a częstotliwość była stała lub była wielokrotnością parzystą. Badania parametrów mikromechanicznych, poprzez nanoindentację, pozwoliły wyznaczyć twardość szkliwa oraz moduł sprężystości (Younga) na powierzchniach koron zębów trzonowych dolnych. Na podstawie charakterystyk wytrzymałościowych i pomiarów ustalono, że twardość zawarta była w przedziale od 337,2 HV do 335,3 HV, a moduł sprężystości w przedziale od 95,8 GPa do 106,3 GPa. Stwierdzono daleko posuniętą regularność w strukturach warstwy wierzchniej szkliwa oraz dużą powtarzalność w badaniach mikromechanicznych.

Słowa kluczowe: szkliwo zębowe, warstwa wierzchnia, chropowatość, mikrotwardość

[Inżynieria Biomateriałów, 102, (2011), 23-27]

Wprowadzenie

Szkliwo stanowi najbardziej wytrzymałą tkankę w ustroju człowieka. Pokrywa ono korony zębów, co decyduje o ich odporności na zużycie tribologiczne, szczególnie przy realizacji funkcji żucia w złożonych warunkach obciążeń okluzyjnych.

THE ANALYSIS OF ENAMEL RESISTANCE TO WEAR DETERMINING FACTORS PART II: STUDY OF SUPERFICIAL LAYER AND MICROHARDNESS IN TOOTH ENAMEL

WOJCIECH RYNIEWICZ¹, MARIOLA HERMAN², ANNA M. RYNIEWICZ^{1,3*}

¹ JAGIELLONIAN UNIVERSITY MEDICAL COLLEGE,
FACULTY OF MEDICINE, DEPARTMENT OF PROSTHETIC DENTISTRY,
4 MONTELUPICH STR., 31-155 CRACOW

² 5TH MILITARY HOSPITAL WITH POLYCLINIC IN CRACOW,
CONSERVATIVE DENTISTRY AND ENDODONTICS WARD,
1-3 WROCŁAWSKA STR., 30-901 CRACOW

³ AGH UNIVERSITY OF SCIENCE AND TECHNOLOGY,
FACULTY OF MECHANICAL ENGINEERING AND ROBOTICS,
30 MICKIEWICZA AV., 30-059 CRACOW

* E-MAIL: GHRYNIEW@CYF-KR.EDU.PL

Abstract

This paper is a continuation of the issues that has pointed determinants deciding about the resistance of natural enamel to wear. Part II contains the examinations including the assessment of enamel superficial layer stereometry using Atomic Force Microscopy (AFM) and determination of teeth microhardness using Oliver & Pharr method.

Statistical analysis of morphologic parameters in enamel from premolar and molar teeth was made using Scanning Probe Image Processor software. The analysis allowed the identification of images with various range of scanning, determination of roughness parameters of the surface in nanoscale and quantitative and qualitative differentiation of the structures. Changes in roughness are periodic, with similar parameters of amplitude, and a frequency can be constant or is an even multiple. Determination of enamel hardness and Young's modulus for the surface of dental crowns in lower molar teeth were possible by micromechanical study using nanoindentation. Based on performance characteristics and measurements it was established, that the hardness ranged from 337.2 HV to 335.3 HV, and Young's modulus ranged from 95.8 GPa to 106.3 GPa. Highly regular pattern in structures of enamel superficial layer and high repeatability in micromechanical examinations were found.

Keywords: tooth enamel, superficial layer, roughness, microhardness

[Engineering of Biomaterials, 102, (2011), 23-27]

Introduction

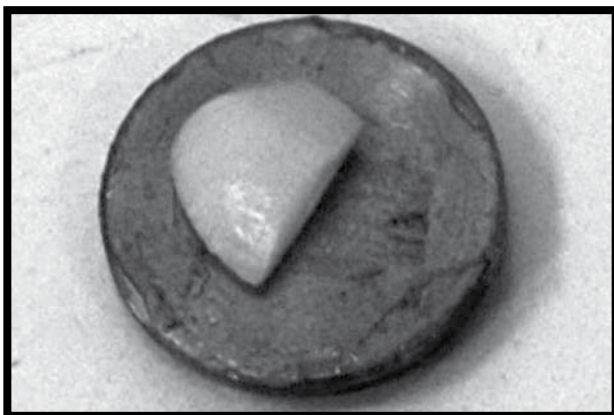
Enamel is the most durable tissue in a human body. It covers dental crowns, which comprise of its resistance to tribological wear, especially during the act of mastication in compound conditions of occlusional loading. Tribological conditions are improved by saliva that moistens dental crowns, and formation of a durable lubricating film is related to the stereometry of enamel superficial layer. AFM was used for a spatial shape examination and the analysis of that layer.

Zwiltowanie koron zębów przez ślinę poprawia warunki tribologiczne, a wytworzenie trwałego filmu smarującego związane jest ze stereometrią warstwy wierzchniej szkliwa. Do badań przestrzennego ukształtowania i analizy tej warstwy wykorzystano AFM. W procesie rozdrabniania kęsów pokarmowych, z równoczesnym zapewnieniem odporności na zużycie, istotną cechą szkliwa jest jego twardość i moduł sprężystości, które wyznaczono z zastosowaniem nanoindentacji.

Celem przeprowadzonych badań była identyfikacja ukształtowania warstwy wierzchniej prawidłowego szkliwa z wykorzystaniem AFM wraz ze statystyczną analizą chropowatości tej powierzchni oraz wyznaczenie mikrotwardości i modułu Younga koron zębów przy użyciu maszyny Scratch Tester CSM Instruments.

Material badań

Materiałem do badań stereometrii warstwy wierzchniej były próbki szkliwa z powierzchni zużywającej zębów przedtrzonowych i trzonowych. Zęby zostały usunięte ze względów ortodontycznych i posiadały prawidłowe szkliwo. Do badań warstwy wierzchniej wytypowano 20 próbek szkliwa (RYS. 1). Do badań mikrotwardości zostało użytych 10 zębów trzonowych dolnych prawidłowo ukształtowanych usuniętych ze względów ortodontycznych. Próbkę przechowywano w soli fizjologicznej, a bezpośrednio przed badaniem stabilizowano woskiem w tulejach badawczych (RYS. 2).



RYS. 1. Próbkę szkliwa przeznaczoną do badań stereometrii warstwy wierzchniej.
FIG. 1. A sample of enamel used for superficial layer stereometric examinations.

Metoda badań

AFM stanowi nowoczesne narzędzie stosowane m.in. do badania powierzchni tkanek i biomateriałów. Technika ta daje możliwość analizy chropowatości powierzchni z niepewnością pomiaru 1 nm i dlatego na obecnym poziomie rozwoju metrologii wydaje się najbardziej przydatną metodą do oceny ukształtowania warstwy wierzchniej [1-4].

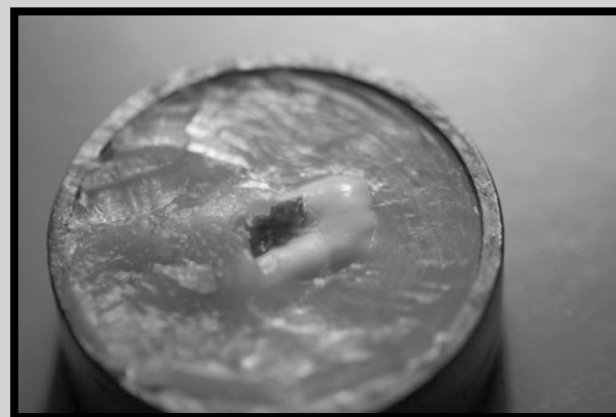
Badania warstwy wierzchniej szkliwa wykonano na mikroskopie sił atomowych NT-NDT sprzężonym z mikroskopem optycznym firmy Olympus (RYS. 3). Mikroskop pracował w trybie bezkontaktowym, który polegał na wykonywaniu pomiarów przy ostrzu odsuniętym od obiektu na odległość 10-100 nm. W tego typu obrazowaniu wykorzystano siły długo zasięgowe, takie jak: siły magnetyczne, elektrostatyczne czy przyciągające siły van der Waalsa.

Hardness and Young's modulus, which were determined using nanoindentation, are essential features of enamel in grinding process of a food morsel with simultaneous providing of resistance to wear.

The aim of conducted examinations was the identification of superficial layer shape of normal enamel, using AFM and statistical analysis of roughness in that surface, and also determination of microhardness and Young's modulus in dental crowns using Scratch Tester CSM Instruments.

Study material

Enamel samples from the masticatory surface of premolar and molar teeth were taken to the stereometric study. The teeth were removed because of orthodontic reasons and they had normal enamel. 20 enamel samples were taken for superficial layer examinations (FIG. 1). 10 lower molar teeth, which had normal structure and were removed because of orthodontic reasons, were used in microhardness examinations. The samples were stored in saline and stabilized in an examination sleeve with wax directly before the examination (FIG. 2).



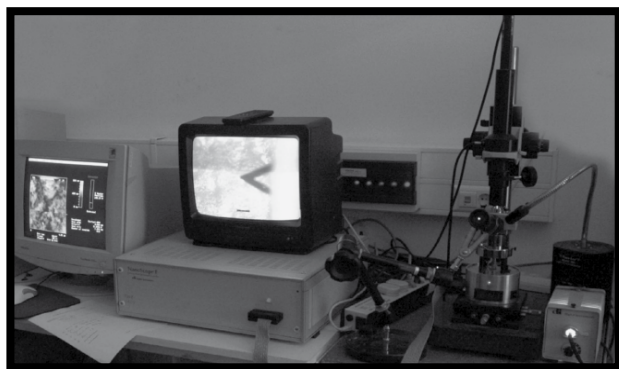
RYS. 2. Ząb stabilizowany woskiem w tulei badawczej do badań wytrzymałościowych.
FIG. 2. A tooth stabilized in an examination sleeve with wax used for strength tests.

Study method

AFM is a modern tool which is used e.g. in examinations of superficial layer of tissues and biomaterials. This technique allows to make an analysis of surface roughness with measurement uncertainty of 1 nm, and therefore it seems to be the most useful method for assessment of superficial layer shape at the present development level of metrology [1-4].

The examinations of enamel superficial layer were conducted using NT-NDT Atomic Force Microscope coupled with Olympus Optical Microscope (FIG. 3). The microscope worked in non-contact mode, and took measurements with a tip-to-sample distance of 10-100 nm. Long range forces were utilized in this imaging modality, such as: electromagnetic, electrostatic and attracting van der Waals forces.

In the examination procedure, a cantilever was set in oscillation with near-resonant frequency by a piezoelectric component. Changes in an amplitude and oscillation frequency were reactions to force acting on the cantilever, and this constituted information which allowed for acquisition of stereometric images of examined superficial layer. Maps of shape of superficial layer in enamel samples were subject of statistical analysis using Scanning Probe Image Processor software for determination of morphologic parameters.



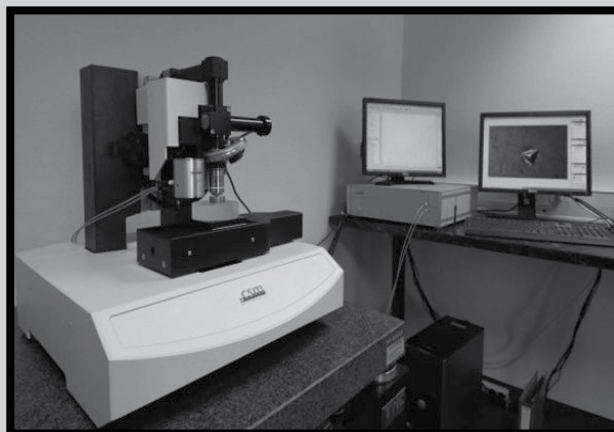
RYS. 3. Stanowisko do badań AFM.
FIG. 3. AFM setup used in examinations.

W zastosowanej procedurze badawczej wprawiano dźwignię w drgania o częstotliwości zbliżonej do częstotliwości rezonansowej za pomocą piezoelementu. Reakcją na siłę działającą na dźwignię była zmiana amplitudy i częstotliwości drgań, co stanowiło informację pozwalającą uzyskać stereometryczne obrazy badanej warstwy wierzchniej. W celu wyznaczenia parametrów morfologicznych mapy ukształtowania warstwy wierzchniej na próbkach szkliva poddano analizie statystycznej z zastosowaniem programu Scanning Probe Image Procesor.

Badania parametrów mikromechanicznych warstwy wierzchniej wykonano poprzez nanoindentację [5,6]. W odróżnieniu od tradycyjnych metod badania twardości, opartych na pomiarze wielkości odcisku powstałego na powierzchni w miejscu penetracji wgłębnika, nanoindentacja pozwoliła rejestrować charakterystykę podczas cyklu obciążania i odciążania wgłębnika. Uzyskana charakterystyka stanowiła podstawę do obliczenia twardości i modułu Younga. Powierzchnie zębów badano metodą Oliver&Pharr na maszynie Scratch Tester CSM Instruments (RYS. 4). Maksymalne obciążenie wgłębnika wynosiło 20 mN, a prędkość obciążania 40 mN/min. Wykonano 10-15 odcisków na powierzchni każdego zęba z użyciem diamentowego indentora Vickersa VG-73.

Wyniki badań i ich omówienie

Na podstawie przeprowadzonych badań uzyskano mapy opisujące ukształtowanie warstw wierzchnich szkliva naturalnego zębów przedtrzonowych i trzonowych (RYS. 5). Topografię badanych powierzchni scharakteryzowano metodą Root Mean Square (RMS) [7] poprzez podanie statystycznych parametrów chropowatości, takich jak S_a (średnie arytmetyczne odchylenie profilu chropowatości od linii średniej), S_q (średnie kwadratowe odchylenie powierzchni – określane od powierzchni odniesienia jako odchylenie standardowe wysokości nierówności powierzchni, $S_q = \text{RMS}$), S_z (maksymalna wysokość chropowatości w obszarze próbkowania). Jednak jak wiadomo, powyższe parametry podlegają prawu skalowania, a więc są ściśle związane z wielkością analizowanego obszaru, zwłaszcza jeżeli rozważany był stan powierzchni na poziomie nano. Na RYS. 6 i 7 zamieszczono mapy i wykresy do statystycznej analizy chropowatości szkliva. Na podstawie tej analizy można wnosić, że zmiany chropowatości szkliva mają charakter okresowy o zbliżonych parametrach amplitudy. Wskazuje na to parametr RMS liczony metodą najmniejszych kwadratów, który w losowo wybranych dziesięciu obszarach ma bardzo zbliżoną wartość (6,017 nm – 7,651 nm). Na podstawie map ukształtowania powierzchni szkliva wyznaczono częstotliwość rozkładów występowania określonych wysokości nierówności (RYS. 8). Uzyskane rozkłady pozwalają stwierdzić dużą regularność w chropowatości powierzchni szkliva.



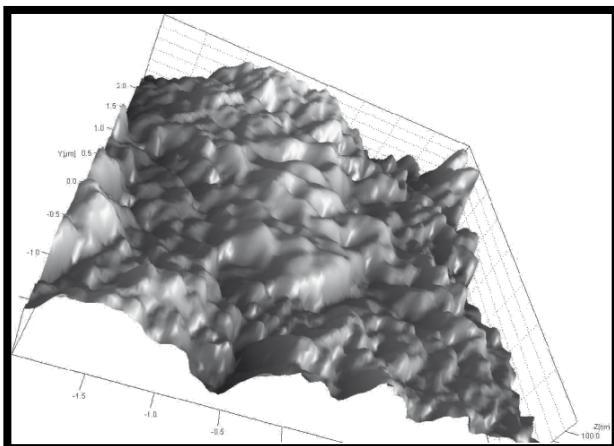
RYS. 4. Stanowisko do badań nanoindentacji.
FIG. 4. A nanoindentation station used in examinations.

A nanoindentation method was utilized to examine micromechanic parameters of superficial layer [5,6]. As opposed to traditional methods of hardness examination, based on a measurement of residual indentation size caused by penetration of a tip on the surface, nanoindentation allows to record characteristics of a load and unload tip cycle. Obtained characteristic was a basis for hardness and Young's modulus calculations. The teeth surface was examined with Oliver & Pharr method using Scratch Tester CSM Instruments (FIG. 4). The maximum load of a tip was 20 mN and a loading rate was 40 mN/min. On the surface of every tooth, 10-15 indentations were made using Vickers VG-73 diamond indenter.

Study results and discussion

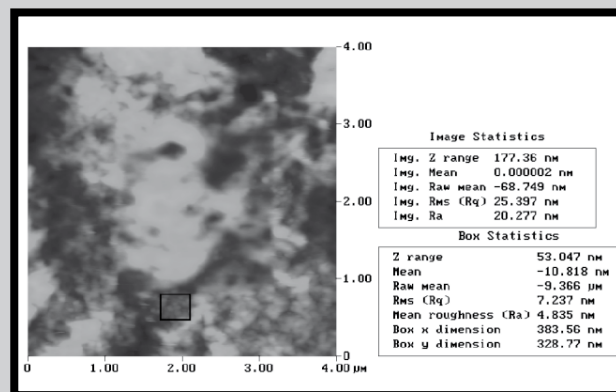
Based on conducted examinations, we have obtained maps describing the shape of superficial layers in natural enamel of premolar and molar teeth (FIG. 5). Examined surfaces topography was described using Root Mean Square (RMS) method [7], by passing statistical parameters of roughness, such as S_a (mean arithmetic deviation of roughness profile from a midline), S_q (mean square deviation of the surface – derived from a reference surface as a standard deviation of irregularity height of a surface, $S_q = \text{RMS}$), S_z (the maximum height of roughness in a sampled area). However, as we know, the above-mentioned parameters are subject to scaling law, so they are strictly bound with an area of analyzed region, especially if a surface condition was considered in nanoscale. In FIG. 6 and 7 there are maps and diagrams for a statistical analysis of glass roughness. We can assume, based on that analysis, that changes of glass roughness are periodic, with similar parameters of amplitude. It is indicated by RMS value, calculated by least squares method, and it has very similar value in ten randomly selected areas (6,017 nm – 7,651 nm). The frequency of distribution of selected heights of roughness was determined based on the shape maps of the enamel surface (FIG. 8). Obtained distributions allowed to find a highly regular pattern in enamel surface roughness.

Microhardness and Young's modulus of a superficial layer in normal teeth were determined based on the analysis of tip imprints and obtained curves. Performed load-unload cycles allowed to obtain characteristics in randomly selected areas of measurement on the superficial layer (FIG. 9).



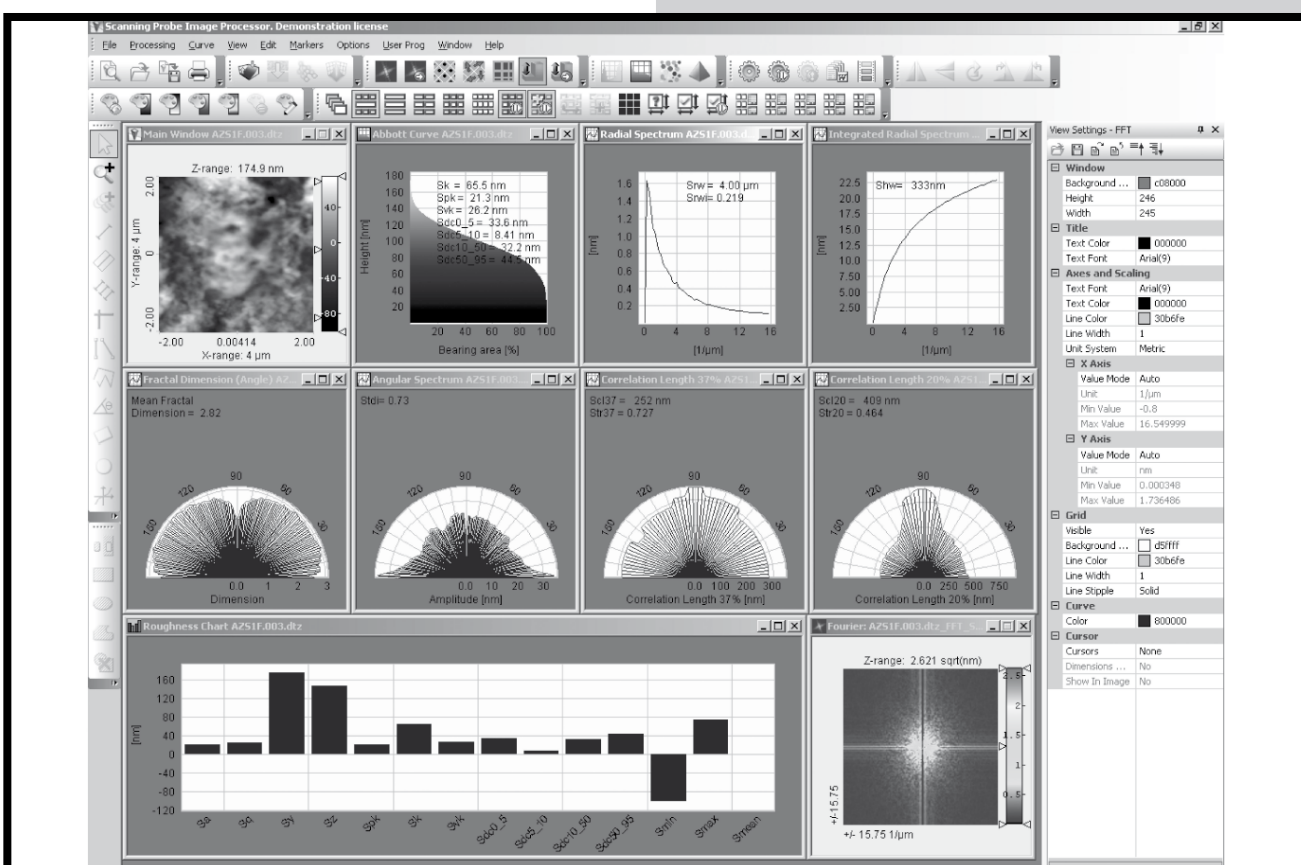
RYS. 5. Przestrzenny obraz prawidłowego szkliwa zębowego z AFM.

FIG. 5. A spatial view of natural enamel obtained by AFM.



RYS. 6. Przykładowa mapa do statystycznej analizy chropowatości szkliwa z zaznaczeniem obszaru ocenianego.

FIG. 6. An example of map used for statistical analysis of glass roughness with marked area for an assessment.

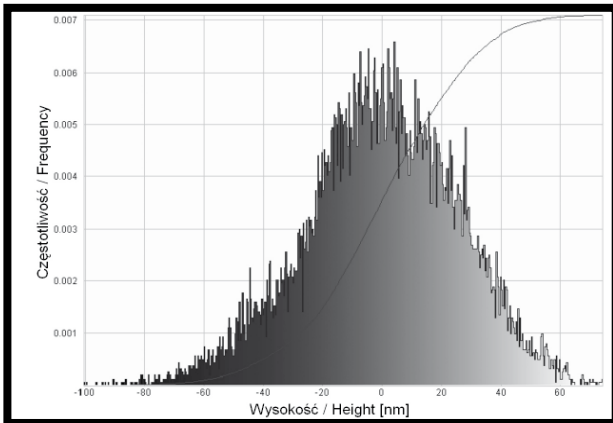


RYS. 7. Parametry warstwy wierzchniej szkliwa prawidłowego.

FIG. 7. Superficial layer parameters of normal enamel.

Mikrotwardość i moduł sprężystości warstwy wierzchniej zębów prawidłowych wyznaczono na podstawie analizy odcisków wgłębnika oraz otrzymanych krzywych. Przeprowadzenie cyklu obciążania i odciążania pozwoliło wyznaczyć charakterystyki w losowo wybranych obszarach pomiarowych warstwy wierzchniej (RYS. 9). Mikrotwardość wyznaczana w trakcie testu była równoznaczna naciskom występującym pomiędzy badaną powierzchnią zęba i wgłębnika diamentowego przy maksymalnym obciążeniu. Moduł sprężystości Younga zależał od właściwości zarówno wgłębnika, jak i badanej struktury zębów. Przy znanych parametrach identora można było ocenić właściwości sprężyste tkanki zębowej. Parametr ten identyfikował tkankę pod względem odpowiedzi sprężystej, której skutkiem była sztywność kontaktowa.

Microhardness determined during the test was equal to pressures which existed between examined tooth surface and a diamond indenter with the maximum load. Young's modulus was dependent upon either of indenter and examined teeth structure properties. Elastic properties of a dental tissue could be assessed with known indenter parameters. This parameter identified a tissue according to its elastic response, resulting in a contact rigidity. Contact rigidity it is essential to food grinding and rubbing processes, and also protects dental crowns from excessive wear [8,9]. Microhardness determined for normal teeth ranged from 337.2 HV to 335.3 HV, and longitudinal elasticity defined by Young's modulus ranged from 95.8 GPa to 106.3 GPa.



RYS. 8. Rozkład wartości wysokości nierówności w warstwie wierzchniej szkliwa prawidłowego w funkcji częstotliwości ich występowania.
FIG. 8. Distribution of irregularity height values of a superficial layer in normal enamel as a function of their incidence.

Szywność kontaktowa ma zasadnicze znaczenie dla procesu rozdrabniania i rozcierania pokarmu, a także zabezpiecza korony zębów przed nadmiernym zużyciem [8,9]. Wyznaczone mikrotwardości zębów prawidłowych zawierały się w przedziale od 337,2 HV do 335,3 HV, a wartości sprężystości wzdłużnej określonej modułem Younga w przedziale od 95,8 GPa - 106,3 GPa.

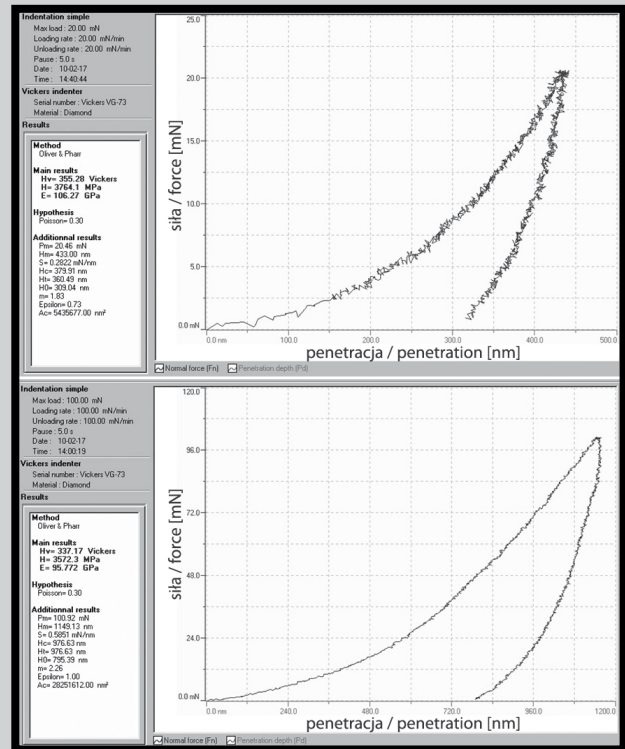
Podsumowanie i wnioski

Mikroskopia AFM jest wiarygodną metodą badawczą w poznaniu właściwości morfologicznych warstwy wierzchniej szkliwa. Na podstawie map otrzymanych z AFM można wyznaczyć przestrzenne obrazy powierzchni oraz przeprowadzić analizę chropowatości warstwy wierzchniej. Analiza statystyczna pozwoliła identyfikować obrazy o różnym zakresie skanowania, wyznaczać parametry chropowatości powierzchni na poziomie nano oraz różnicować struktury w sposób jakościowy i ilościowy. Zmiany chropowatości miały charakter okresowy o zbliżonych parametrach amplitudy, a częstotliwość była stała lub stanowiła wielokrotność parzystą. Taki regularny obraz warstwy wierzchniej będzie sprzyjał tworzeniu filmu smarnego na koronie zęba, a w kontakcie z zębem przeciwnym powstaną warunki do tworzenia nanoklinów, które mogą zapobiegać nadmiernemu zużyciu powierzchni okluzyjnych. Analiza obrazów przestrzennych szkliwa zębego pozwala stwierdzić daleko posuniętą regularność w strukturach warstwy wierzchniej.

Wysoka mikrotwardość szkliwa oraz wysokie wartości modułu sprężystości zabezpieczają odpowiednią szywność kontaktową, co przekłada się na optymalne warunki do rozgniatania i rozcierania kęsów pokarmowych z równoczesną odpornością na zużycie.

Piśmiennictwo

- [1] Drelich J., Tormoen G.W., Beach E.R.: Determination of solid surface tension from particle – substrate pull – off forces measured with the atomic force microscope, *Journal of Colloid and Interface Science*, 2004, vol. 280, 484-497.
- [2] Lehenkari P.P., Charras G.T., Nykanen A., Horton M.A.: Adapting atomic force microscopy for cell biology, *Ultramicroscopy* 2000, 82, 289.
- [3] Mainsah E., Greenwood I.A., Chetwynd D.G.: *Metrology and properties of engineering surfaces*, Kluwer Academic Publisher, 2001.
- [4] Vie V., Giocondi M.C., Leśniewska E. et. al.: Tapping – mode atomic force microscopy on intact cells: optimal adjustment of tapping conditions by using the deflection signal, *Ultramicroscopy* 2000, 82, 279.



RYS. 9. Przykładowe charakterystyki wytrzymałościowe dla zębów prawidłowych.
FIG. 9. An example of strength characteristics for normal teeth.

Conclusions

AFM is a reliable study method, which is utilized in learning of morphologic properties of enamel superficial layer. Based on maps obtained from AFM, it is possible to make spatial images of the surface and conduct the analysis of superficial layer roughness. Statistical analysis allowed the identification of images with various range of scanning, determination of roughness parameters of the surface in nanoscale and quantitative and qualitative differentiation of the structures. Changes in roughness are periodic, with similar parameters of amplitude, and a frequency can be constant or is an even multiple. Such a regular image of superficial layer will support formation of lubricating film on dental crowns, and by contact with opposite tooth, it will create conditions to nano-wedge formation, which can prevent from excessive wear of occlusal surfaces. The analysis of spatial images of tooth enamel allowed us to identify a highly regular pattern in the superficial layers.

High microhardness of enamel and high values of Young's modulus protect an appropriate contact rigidity, which results in optimal conditions to crush and rub food morsels and resistance to wear at the same time.


References

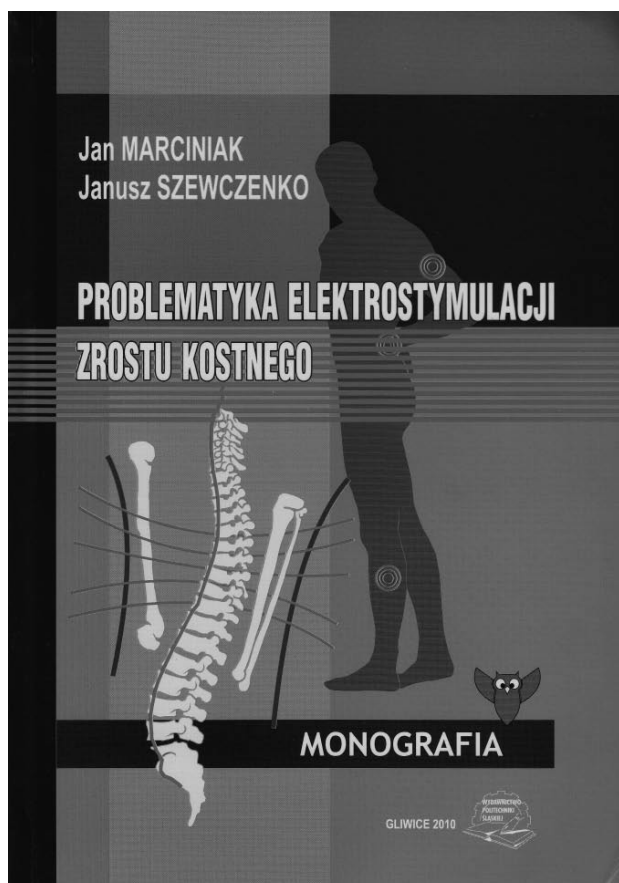
- [5] Cuy J. et al. „Nanoindentation mapping of mechanical properties of human molar tooth enamel” *Arch. Oral Biology*, 2002 (474) 281-291.
- [6] Habelitz S. et al. „Mechanical properties of human dental enamel on the nanometre scale”, *Archives of Oral Biology* 46 (2001) 173-183.
- [7] Wiercokowski M., Cellary A., Chajda J.: *Przewodnik po pomiarach nierówności powierzchni czyli o chropowatości i nie tylko*, Wyd. Politechniki Poznańskiej, Poznań 2003.
- [8] Ryniewicz W., Ryniewicz A. M. „Modelowanie mechaniki kontaktu filarów i uzupełnień protetycznych metodą elementów skończonych” *Implantoprotetyka* 2004 (913) 31-36.
- [9] Las Casas E.B. et al. „Enamel wear and surface roughness characterization using 3D profilometry” *Tribology International* 2008 (41) 1232-1236.

.....

STUDIA PODYPLOMOWE

Biomateriały – Materiały dla Medycyny

| | | |
|--|--|---|
| Organizator: Akademia Górniczo-Hutnicza Wydział Inżynierii Materiałowej i Ceramiki Katedra Biomateriałów Kierownik: Dr hab. inż. Elżbieta Pamuła | Adres: 30-059 Kraków, Al. Mickiewicza 30 Pawilon A3, p. 108 lub 107 tel. 12 617 44 48, 12 617 34 41; email: epamula@agh.edu.pl stodolak@agh.edu.pl |  |
| http://www.agh.edu.pl/pl/studia/studia-podyplomowe/biomateriały-materiały-dla-medycyny.html | | |
| Charakterystyka: Tematyka prezentowana w trakcie zajęć obejmuje przegląd wszystkich grup materiałów dla zastosowań medycznych: metalicznych, ceramicznych, polimerowych, węglowych i kompozytowych. Studenci zapoznają się z metodami projektowania i wytwarzania biomateriałów a następnie możliwościami analizy ich właściwości mechanicznych, właściwości fizykochemicznych (laboratoria z metod badań: elektronowa mikroskopia skaningowa, mikroskopia sił atomowych, spektroskopia w podczerwieni, badania energii powierzchniowej i zwilżalności) i właściwości biologicznych (badania: in vitro i in vivo). Omawiane są regulacje prawne i aspekty etyczne związane z badaniami na zwierzętach i badaniami klinicznymi (norma EU ISO 10993). Studenci zapoznają się z najnowszymi osiągnięciami medycyny regeneracyjnej i inżynierii tkankowej. | | |
| Czas trwania: 1 semestr - letni, 7 zjazdów (soboty-niedziele) co 2 tygodnie, początek zajęć: 25.02.2012. Przewidywana liczba godzin: 120, rozpoczęcie rekrutacji: 1.10.2011, Wymagane dokumenty: dyplom ukończenia szkoły wyższej. | | |



„Problematyka elektrostymulacji zrostu kostnego”

Autorzy: Jan Marciniak, Janusz SzeWCzenko

Wydawnictwo Politechniki Śląskiej

Rok wydania: 2010

Monografia obejmuje syntezę najnowszych informacji oraz własnych doświadczeń klinicznych z obszaru stymulacji zrostu kostnego prądami elektrycznymi. Te doświadczenia nawiązują do poszukiwania efektywniejszych metod aktywizowania zrostu kostnego i przywracania tkankom strefy urazu prawidłowych struktur i utraconych funkcji. Rozwiązania bazują na biofizycznych możliwościach wynikających z własności elektrycznych kości oraz oddziaływania impulsów elektrycznych na procesy metaboliczne w tkance kostnej.

W treści monografii ujęto rozwój i modyfikacje technik leczenia złamań i rekonstrukcji układów kostno-stawowych weryfikowanych klinicznie. Uwypuklono również czynniki, które przyczyniły się do aktywacji procesu gojenia złamań kości. Wskazane zostały metody i parametry elektrostymulacji. Omówiono też urządzenia stosowane do prowadzenia elektrostymulacji różnymi metodami z wykorzystaniem skutecznych przebiegów prądowych aktywizacji i działania przeciwbólowego. Wiele uwagi poświęcono kwestii bezpieczeństwa. Monografia znakomicie wypełnia lukę na krajowym rynku wydawniczym z zakresu: ortopedii, traumatologii, jak i rehabilitacji i będzie szczególnie przydatna dla słuchaczy studiów dziennych, podyplomowych i doktorskich, czy kursów aktualizacji wiedzy lekarzy oraz słuchaczy na uczelniach medycznych i technicznych na kierunkach inżynierii biomedycznej.

.....